

ABSTRACT

Title of Document: MULTIPLEXED CHEMICAL SENSING AND
THIN FILM METROLOGY IN
PROGRAMMABLE CVD PROCESS.

Yuhong Cai, Doctor of Philosophy, 2005

Directed By: Professor Gary W. Rubloff,
Department of Materials Science and
Engineering and the Institute for Systems
Research

Mass spectrometry (mass spec) has proven valuable in understanding and controlling chemical processes used in semiconductor fabrication. Given the complexity of spatial distributions of fluid flow, thermal, and chemical parameters in such processes, multi-point chemical sampling would be beneficial.

This dissertation discusses the design and development a multiplexed mass spec gas sampling system for real-time, *in situ* measurement of gas species concentrations in a spatially programmable chemical vapor deposition (SP-CVD) reactor prototype, where such chemical sensing is essential to achieve the benefits of a new paradigm for reactor design. The spatially programmable reactor, in which across-wafer distributions of reactant are programmable, enables (1) uniformity at any desired process design point, or (2) intentional nonuniformity to accelerate process optimization through combinatorial methods. The application of multiplexed mass spec sensing is well suited to our SP-CVD design, which is unique in effectively segmenting the showerhead gas flows by using exhaust gas pumping through the

showerhead for each segment. In turn, mass spec sampling signals for each segment are multiplexed to obtain real-time signatures of reactor spatial behavior. In this dissertation, we have reported the results using inert gases to study the spatial distributions of species, validate SP-CVD reactor models, and lead to an understanding of fundamental phenomena associated with the reactor design.

This novel multiplexed mass spec sensing system has been employed to monitor the process among three segments in real time. Deliberate non uniform W SP-CVD was performed using H₂ reduction of WF₆. A process based metrology, which reflects the relationship between the process recipe and film thickness was established. From the process based metrology, a recipe for uniform film deposition was determined and the re-programmability of the SP-CVD system was proven. Meanwhile, a mass spec sensor based film thickness metrology, which reflects the relationship between the normalized mass spec signal and film thickness, was built. Mass spec sensor based thickness metrology with precision of 2~4% was obtained, approaching the desired range of thickness control precision.

The scientific contributions from this work are summarized as two points: (1) spatially resolved *in situ* sensing metrologies have been developed for real-time advanced process control; and (2) the results of this sensing methodology not only demonstrates real-time spatially-distributed end point control, but also makes it possible to guide rapid reprogramming of process recipes intended to achieve simultaneous high material quality and uniformity, or to serve as a valuable asset to potential combinatorial experimental capabilities of the SP-CVD reactor.

MULTIPLEXED CHEMICAL SENSING AND THIN FILM METROLOGY IN
PROGRAMMABLE CVD PROCESS

By

Yuhong Cai

Dissertation submitted to the Faculty of the Graduate School of the
University of Maryland, College Park, in partial fulfillment
of the requirements for the degree of
Doctor of Philosophy
2005

Advisory Committee:
Professor Gary W. Rubloff, Chair
Professor Raymond A. Adomaitis
Professor Robert M. Briber
Professor Isabel K. Lloyd
Professor Mohammad Al-Sheikhly

© Copyright by
Yuhong Cai
2005

Dedication

To my father, mother and husband whom I love the most.

Acknowledgements

Ramaswamy Sreenivasan, Dr. Jae-Ouk Choo, Laurent Henn-Lecordier, Jing Chen, Wei Lei, Erin Robertson, and Rinku P. Parikh for support in experimental works, data analysis, and result discussion.

Dr. Robert Ellefson, Dr. Louis Frees, Kenneth A. Rosys, David Rayle, and Peter.Schubert (Inficon) for the equipment supply and beneficial discussion.

Table of Contents

Dedication.....	ii
Acknowledgements.....	iii
Table of Contents.....	iv
List of Tables.....	vi
List of Figures.....	vii
Chapter 1: Introduction.....	1
1.1 Function of advanced process control (APC).....	1
1.2 Motivation.....	2
1.2.1 Importance of <i>in situ</i> chemical sensors.....	2
1.2.2 Value of multi-point sensing.....	2
1.2.3 Types of chemical sensors.....	3
1.2.4 Benefit of using real-time mass spec APC.....	4
1.3 Research objectives.....	5
1.4 Problems and challenges in this research.....	6
1.4.1 Pressure transduction.....	6
1.4.2 Multiplexed chemical sensing applications for process monitor and control.....	7
Chapter 2: Spatially programmable chemical vapor deposition system.....	12
2.1 Chemical vapor deposition.....	12
2.2 Tungsten CVD.....	14
2.3 Spatially Programmable CVD (SP-CVD) concept.....	15
Chapter 3: Design and implementation of multiplexed mass spec sensing in SP-CVD.....	23
3.1 Real time APC with in situ sensing for process metrology and process control.....	23
3.2 Multi-point mass spec sensing.....	23
3.3 Pressure transduction strategy for gas sampling.....	24
3.3.1 Mass spec and pressure reduction requirements.....	24
3.3.2 Simulation model for pressure reduction design.....	24
3.4 Multiplexed gas sampling system design.....	27
3.4.1 Using the mass spec for sampling of the three segments.....	27
3.4.2 Using the mass spec for process fault detection and contamination control.....	29
3.5 Mass spec signal integration.....	30
Chapter 4: Gas distribution and gas transportation mechanisms in SP-CVD reactor.....	38
4.1 Mechanisms of inter-segment gas diffusion.....	38
4.2 Quantify the contribution of signal from ISM-wafer and ISM-BD.....	40
4.3 Concentration profiles along vertical showerhead segments.....	41
Chapter 5: SP-CVD experimental procedure.....	51
5.1 Methodology.....	51
5.2 Training experiments to build metrologies.....	53
5.3 Demonstration of programmability --- uniform film deposition.....	58

Chapter 6: Discussion	68
6.1 Use inter-segment gas diffusion to control the deposition gradient	68
6.2 Mass spec signal variation in the different segment	69
6.3 Transient peak in the mass spec signal	70
6.4 Non-uniform heating effect and programmability of SP-CVD	71
6.5 Sensor based metrology vs. process based metrology	72
6.6 The accuracy of end point control	73
Chapter 7: Conclusion and future work	81
7.1 Multiplexed mass spec sensing in SP-CVD.....	81
7.2 Multiplexed mass spec based thickness metrology and process control	82
Bibliography.....	84

List of Tables

Table 3- 1	Valve operation of the mass spectrometry sampling system.....	32
Table 4- 1	Gas flow rates in three segments.	44
Table 5- 1	Deliberate non uniform W film deposition recipes and thickness measurement	59
Table 5- 2	Comparison of the average uncertainty and standard deviation obtained from two metrologies.	60
Table 5- 3	Uniform W film deposition recipe and thickness measurement.....	61
Table 6- 1	Transient time for different gases	76
Table 6- 2	SP-CVD end point detection experiment data and statistical analysis results.	77

List of Figures

Figure 1- 1	Real time mass spec APC	9
Figure 1- 2	Chronological order of experimentation to establish mass spec based metrology	10
Figure 1- 3	Structure of mass spec	11
Figure 2- 1	Chemical vapor deposition (CVD) reaction	18
Figure 2- 2	Programmable CVD reactor design	19
Figure 2- 3	Front view of programmable CVD chamber mechanical design.....	20
Figure 2- 4	Spatially programmable chemical vapor deposition (SP-CVD) system.	21
Figure 2- 5	Gas flow in the SP-CVD reactor.	22
Figure 3- 1	Bottom view of the programmable CVD showerhead.....	33
Figure 3- 2	Schematic of pressure reduction in the mass spec sampling system. .	34
Figure 3- 3	Schematic diagram of multiplexed mass spec sampling system.....	35
Figure 3- 4	Mass spec signal separation.	36
Figure 3- 5	SP-CVD mass spec sensing VI front panel.....	37
Figure 4- 1	Two types of inter-segment gas mixing	45
Figure 4- 2	QMS signal validates the recirculated gas flow in programmable CVD showerhead.	46
Figure 4- 3	Quantify contribution of H ₂ signal from inter-segment gas diffusion	47
Figure 4- 4	Gas composition at the different positions in segment-2 with a 1mm gap size between the showerhead and the wafer surface.....	48
Figure 4- 5	Gas composition in mole fraction in segment-2 (experimental result and simulation data), the Std. of experimental data is within 0.3%~0.4%.....	49
Figure 4- 6	Ar and H ₂ mass spec signal as a function of position in segment-2 when feeding the same gas in three segments.	50
Figure 5- 1	Non-uniform W film deposition.....	62
Figure 5- 2	Linear statistic model between W film thickness and square root of H ₂ mole fraction.	63
Figure 5- 3	H ₂ , HF and WF ₆ mass spec signals from a typical programmable W CVD process. Monitoring time: 20 sec/segment; 60 sec/cycle. Typically, there are 15 cycles of monitoring during the process. This figure only illustrates the first 4 cycles of mass spec monitoring signals.	64
Figure 5- 4	<i>In situ</i> HF generation signal obtained in programmable W CVD process. A, B, C, D present the HF signal integration value from the 1 st four cycles in segment 2.	65
Figure 5- 5	W film thickness vs. normalized time integration of HF mass spec signal. (a) Metrology results in segment 1; (b) Metrology results in segment 2; (c) Metrology results in segment 3.....	66
Figure 5- 6	Uniform W film deposition.....	67
Figure 6- 1	Mass spec signal from different segment.....	78
Figure 6- 2	Plots showing target thickness data from sensor based metrology vs.	

	experimental thickness data measured by 4PP after the experiments were stopped by end pointing using multiplexed mass spec for 5 wafers.....	79
Figure 6- 3	Substrate heater: more heater coils in segment-2 area.....	80

Chapter 1: Introduction

1.1 Function of advanced process control (APC)

Semiconductor manufacturing has faced increasing pressure to improve process efficiency and flexibility, meanwhile, decreasing production costs. Without making significant changes to the production process and equipment, improvement can be made by applying advanced process control (APC) technology in the manufacturing process. APC is a methodology used to determine when and how to make adjustments so that the process output remains on target.^{1, 2, 3, 4} Course correction and fault management are the two main components of APC technology.¹

Using a metrology method to maintain process reproducibility is defined as course correction. Course correction has been used for both run-to-run control and real-time control.¹ In a run-to-run controlled process, the sensor measures, collects and analyzes the data, as well as calculates new settings for the next run. Therefore, a run-to-run process can use in situ and ex situ measurements to correct systematic process drifts.

Fault management includes fault detection and fault diagnosis. Fault detection registers an alarm when an abnormal condition develops in the monitored process or system. Once a fault is detected, the process/systems engineer can identify the root cause of the abnormality and implement corrective action before more wafers are degraded.⁵

1.2 Motivation

1.2.1 Importance of *in situ* chemical sensors

Real-time, *in situ* chemical sensing has played an important role in advanced process control (APC) in the semiconductor industry.^{1,2,6} Understanding and controlling these processes are the two primary motivations of applying *in situ* chemical sensing in semiconductor processes.⁷ From a manufacturing efficiency point of view, production yield and capital equipment productivity can be significantly improved through direct process monitoring and real-time process control of gas phase composition.¹ Ideally, an effective process sensor can provide direct information regarding deposition kinetics as well as information on nominal process parameters, such as gas flow rate, process pressure and reaction time.⁵ In such cases, the sensor can reflect equipment state, process state, and wafer state, providing an avenue to both course correction and fault management, the two thrusts of advanced process control.¹

1.2.2 Value of multi-point sensing

Multi-point chemical sensing is a method by which multiple sensors are spatially dispersed to collect signals from several spatially separated points in chemical processes such as chemical vapor deposition (CVD) or atomic layer deposition (ALD). Compared to single-point sensing technology, multi-point chemical sensing offers the potential of greater understanding and control of three-dimensional process behavior and its consequences across the wafer. Our recent research has been focused on:

- Development and demonstration of a spatially programmable CVD (SP-CVD) reactor design;
- A new paradigm for process equipment generally and for CVD equipment specifically.

This approach has promise to control the spatial profile of gas composition across the wafer surface, and thereby to achieve uniformity or to intentionally introduce nonuniformities in pursuit of combinatorial process studies. Real-time multi-point sensing is particularly useful in programmable CVD, not only to detect spatial variations in process conditions, but also to drive control through the spatial programmability of the SP-CVD reactor design. This should be valuable in achieving real-time end point control at multiple locations across the wafer, or for other approaches, which tailor spatial distributions through the process cycle.

1.2.3 Types of chemical sensors

Several techniques have been developed for *in situ* process monitoring,^{8, 9, 10} including Fourier transform infrared spectroscopy (FTIR),^{11, 12, 13} acoustic sensing^{14, 15} and quadrupole mass spectrometry (QMS).^{16,17,18} We concentrate here on QMS because of its ability to detect both reactant and product species, to use for metrology and control (discussed in Chapter 5), and to exploit the fact that QMS sensors are already present for fault detection on many manufacturing process tools (described in Chapter 3.4.2).

QMS ionizes atoms or molecules from a sample and then separates them according to their *mass-to-charge ratio*.¹⁹ Traditional applications of QMS include: vacuum system leak detection and monitoring of residual gas distributions for

contamination control.^{20, 21} More advanced applications of QMS have been demonstrated by several research groups.^{22, 23} Greve's group used mass spectrometry (mass spec) for process control²⁴ and for real-time multivariable control of PECVD SiN film properties.²⁵ T. Gougousi *et al.* applied QMS to run-to-run control on a W-CVD cluster tool.²⁶ Xu *et al.* successfully demonstrated QMS-based thin film thickness metrology and end point control in a tungsten chemical vapor deposition (W CVD) process.^{27, 28}

In this work, we have extended QMS sensing to incorporate multiplexing of the sensor to sample various segments of a segmented showerhead, which is the key feature of the SP-CVD reactor. This makes possible experimental validation of fluid flow models essential to process control in the context of the programmable reactor concept. It also enables quantitative monitoring of deposition on the wafer associated with each showerhead segment, leading to film thickness metrology and real-time end point control. In this dissertation, we report the results of:

- Using inert gas mixtures (which is a standard approach) to understand and improve our models of the programmable CVD reactor and to develop the multiplexed QMS technology.
- Applying the programmable reactor concept to demonstrate both uniformity control and combinatorial experimentations in W CVD process.

1.2.4 Benefit of using real-time mass spec APC

Within the three segments, across-wafer impingement is programmable in order to achieve uniformity or to intentionally introduce non-uniformities in the run-to-run control process. However, with the use of an *in situ* mass spec sensor to

monitor and control the SP-CVD process in real time (as shown in Figure 1- 1), greater flexibility can be introduced into the programmable CVD process. For instance, the thickness target can be changed during the deposition process and a film with a new target thickness can be obtained without wasting wafers or precursors. This method offers the benefit of a faster turn around time during the process.

Figure 1- 2 explains the chronological order of experimentation to establish mass spec based metrology. After building the SP-CVD reactor and multiplexed mass spec sampling system, non-uniformity depositions were conducted as training experiments in order to build film thickness metrology. At the same time, the mass spec was used to monitor the process and collect the signal of reactant and byproduct gases within the system. Post-process characterization was performed by a 4-point-probe measurement to determine the film thickness. Thereafter, two metrologies to the SP-CVD process control were developed: (1) a process based metrology, which reflects the relationship between the reactant gas concentration and film thickness in each segment; (2) a mass spec sensor based metrology, which reflects the relationship between the normalized mass spec signal and the film thickness in each segment. Finally, the process based metrology was employed to reprogram the process and deposit a uniform film across the wafer. Furthermore, the sensor based metrology was applied to conduct real-time end point control in W SP-CVD.

1.3 Research objectives

There are four research objectives:

(1) Design and develop a multiplexed and multipoint mass spec sampling system to provide *in situ* measurement of the spatial distribution of gas composition above wafer surface.

(2) Use the mass spec as a distributed chemical sensor to evaluate and improve the models of SP-CVD equipment and process.

(3) Develop a thin film thickness metrology by establishing a model between the film thickness and the mass spec signal integrated over the deposition time.

(4) Apply the thickness metrology to achieve real-time process control and process end point detection and control, which lead to efficient process development, process optimization and combinatorial process studies.

1.4 Problems and challenges in this research

As described earlier, we use the mass spec as a real-time *in situ* chemical sensor to monitor and control the CVD process. The main technical challenges in this research are described in the following sections.

1.4.1 Pressure transduction

Mass spec is chemical sensing instrument comprising three physically important sub-systems: the ion source, mass filter (quadrupole separation system) and ion detector (Figure 1- 3). Mass Spec ionizes atoms or molecules from a sample, separates the different gas ions according to their *mass-to-charge ratio* (m/z),²⁹ and measures the masses and relative concentrations of molecules. The ions of different mass are separated by controlling the travel paths of the ionized sample molecules. The ions should pass through the spectrometer system without collisions with other

molecules or other ions; deflection with other ions causes them to deviate from the path that the electric fields are directing them³⁰. Inficon mass spectrometer's operation pressure is required to be lower than 10^{-5} Torr;^{31,32} however, the programmable CVD process is at 1 Torr region. One of the big challenges in the mass spec sampling system is to design a process specific inlet system which makes mass spec have the capability of monitoring high pressure process.

1.4.2 Multiplexed chemical sensing applications for process monitor and control

Mass spec are fairly expensive process analyzers.³⁰ Cost reduction is one of the biggest concerns in implementing advanced process control in manufacturing. The question is: can we use one chemical sensor to monitor the reaction rates in the different segments nearly simultaneously, so that the result approximates multi-channel real-time chemical sensing. There are three segments in programmable CVD reactor; each segment experiences different CVD recipes with different parameter settings, such as, different gas flow rates, different precursors and different temperatures. In order to monitor the gas concentration in each of three segments during a single deposition process quite frequently, it is necessary to switch the sensor between segments. This cyclic switching is henceforth referred as multiplexed process monitoring. However, the monitoring time for each segment is limited by the gas transfer time of the process monitor. We defined the gas transfer time as the time taking the process gas from the CVD reaction chamber to the mass spec sensor. If the monitoring time is less than gas transfer time, then the data shown on the mass spec cannot reflect the real-time process status. But if we set a long monitoring time, we will not have enough data point. For this reason, we should consider the tradeoff

between the monitoring time and the gas transfer time when we design the sampling inlet system and the parameters for the monitoring switch of the segment.

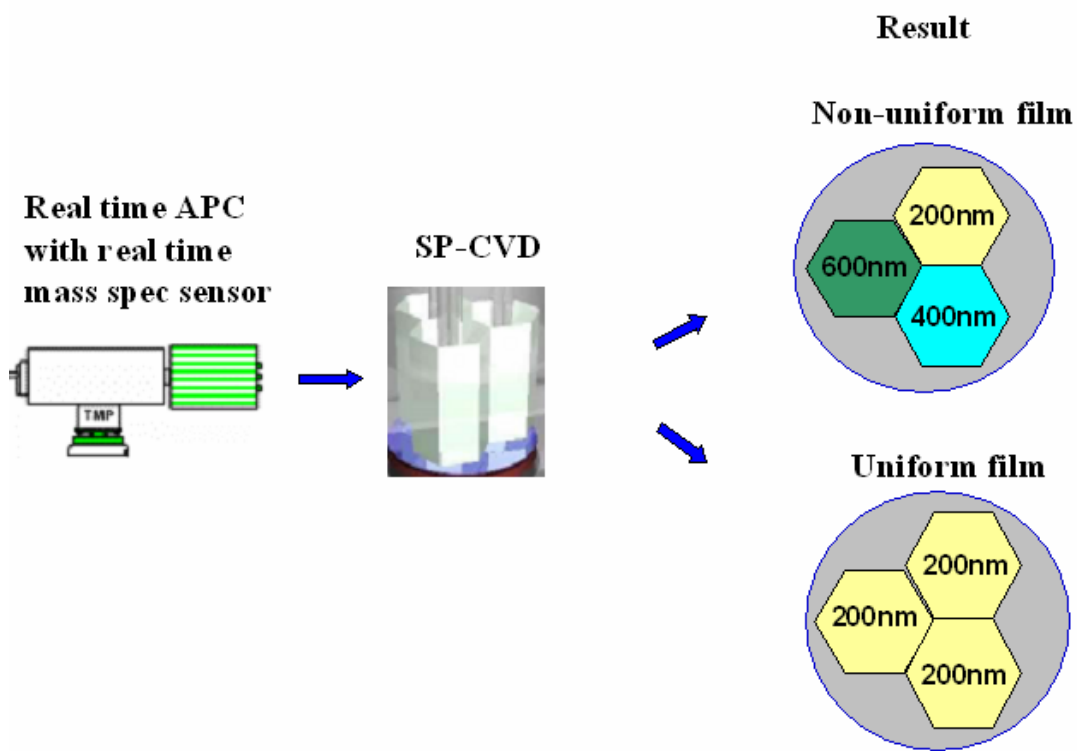


Figure 1- 1 Real time mass spec APC

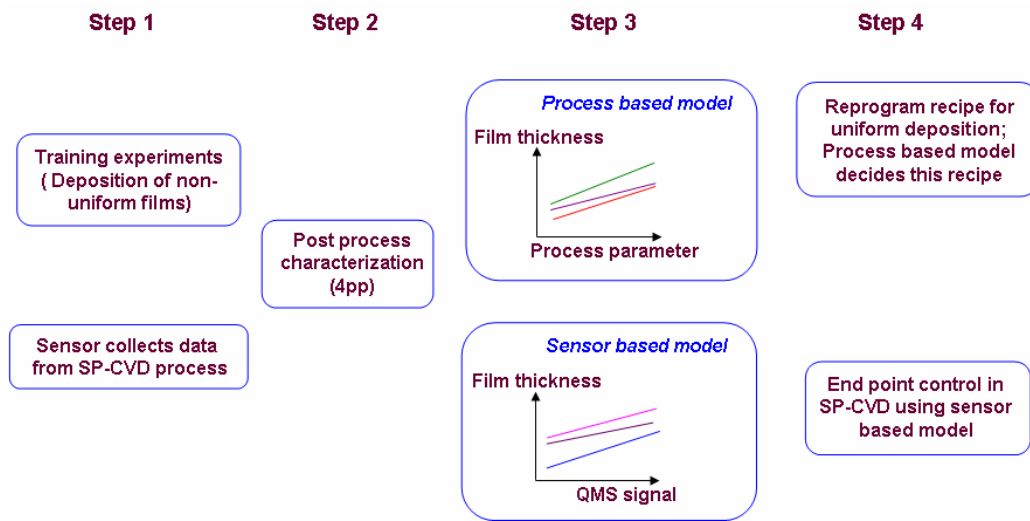


Figure 1- 2 Chronological order of experimentation to establish mass spec based metrology

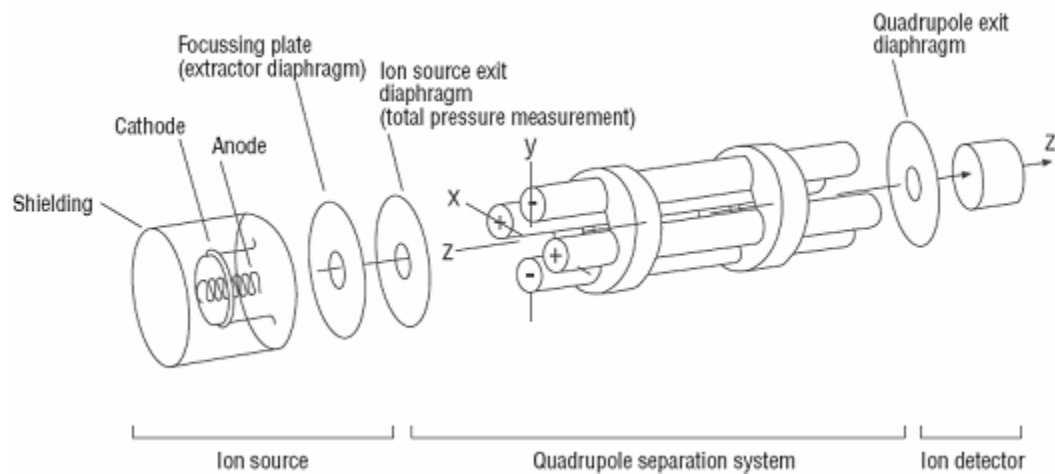


Figure 1- 3 Structure of mass spec

Chapter 2: Spatially programmable chemical vapor deposition system

2.1 Chemical vapor deposition

Chemical vapor deposition (CVD) is a chemical process for depositing thin films of various materials on a substrate. Compared to other thin film deposition technologies such as thermal evaporation, sputtering, pulsed laser deposition (PLD), electron beam evaporation (E-beam) and molecular beam epitaxy (MBE), it offers good control of film composition, step coverage, film uniformity, as well as excellent growth rates. Therefore, CVD is widely used in the semiconductor industry,^{33, 34} as part of the semiconductor device fabrication process, to deposit various films including: polysilicon, tungsten, silicon nitride, titanium nitride, silicon dioxide, silicon germanium and various high-k dielectrics. Figure 2- 1 depicts the basic steps in a typical CVD reaction:

1. Transport of precursor molecules into reactor;
2. Adsorption of precursor molecules to substrate;
3. Chemical reaction and form solid films;
4. Recombination of molecular byproducts and desorption into gas phase.

There are various forms of CVD processes, including:

1. Atmospheric pressure CVD (APCVD) - CVD process is at atmospheric pressure.

2. Low-pressure CVD (LPCVD) - CVD process is at subatmospheric pressures and high temperature.
3. Ultra-high vacuum CVD (UHVCVD) - CVD processes at very low pressures, typically in the range of a few to a hundred millitorrs. Most modern CVD process is either LPCVD or UHVCVD.
4. Plasma-enhanced CVD (PECVD) - CVD processes that utilize plasma to enhance chemical reaction rates of the precursors. PECVD processing allows deposition at lower temperatures, which is often critical in the manufacture of semiconductors.
5. Atomic layer CVD (ALD) - A CVD process in which two complementary precursors are alternatively introduced into the reaction chamber. One of the precursors will adsorb onto the substrate surface, but cannot completely decompose without the second precursor. The precursor adsorbs until it saturates the surface and further growth cannot occur until the second precursor is introduced. The film thickness is controlled by the number of precursor cycles rather than the deposition time. ALD is very good for extremely precise control of film thickness and uniformity.
6. Metal-organic CVD (MOCVD) - CVD processes based on metal-organic precursors.
7. Rapid thermal CVD (RTCVD) - CVD processes that use heating lamps or other methods to rapidly heat the substrate. Heating only the substrate rather than the gas or chamber walls helps reduce unwanted gas phase reactions that can lead to particle formation.

Reducing pressure in CVD process can reduce unwanted gas phase reactions and improve film quality (purity, uniformity across the wafer). In this research, we select LPCVD process to produce W thin film in a spatially programmable CVD reactor at a high temperature ~ 400°C.

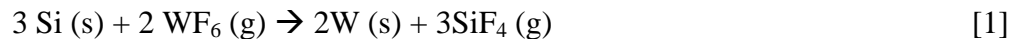
2.2 Tungsten CVD

In the last decade, the tungsten chemical vapor deposition using tungsten hexafluoride (WF_6) is a very active research area in ultra large scale integrated (ULSI) fabrication. The attractive feature of tungsten CVD is the possibility of filling contact holes and vias. For example, deposition of pure tungsten can be used to fill the holes that make contact to the transistor source and drain ("contact holes") and also to fill vias between successive layers of metal. This approach is known as a "tungsten plug" process.

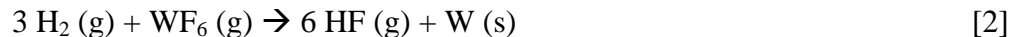
The basic chemical reaction is the reduction of the WF_6 molecule, depositing the tungsten and removing the fluorine atoms through a volatile reaction product.³⁵ One of the most common processes uses WF_6 as the tungsten precursor and H_2 as the reducing agent.^{36, 37}

The deposition process includes two steps:³⁸

Step 1: Si reduction of WF_6 .



Step 2: H_2 reduction of WF_6 :



In step 1, WF_6 is reduced by reaction with the silicon substrate, which typically results in the formation of a “nucleation layer” approximately 300Å thick.^{39, 40} The thickness of the seed layer can vary considerably from sample to sample, but it appears to be dependent on the amount of native oxide which remains on the surface prior to deposition.⁴¹ On this tungsten nucleation layer, WF_6 further reacts with H_2 and deposits solid W film.⁴² In step 2, three moles of H_2 and one mole of WF_6 can produce six moles of HF and one mole of W film. In general, the hydrogen reduction process is capable of producing conformal film coverage on submicron features of aspect ratio > 1 .^{43, 44, 45}

2.3 Spatially Programmable CVD (SP-CVD) concept

Spatially Programmable CVD (SP-CVD) system design has the potential to overcome shortcomings in conventional CVD equipment, including: (1) difficulty to control thin film uniformity across the wafer surface; (2) equipment flexibility to allow optimization of material quality and uniformity simultaneously.⁴⁶

The programmable CVD system has been built based on a new paradigm of equipment aimed at achieving distributed sensing and spatial control of process parameters. In the case of CVD, we achieve this through a reactor design,⁴⁷ which employs a segmented gas injection showerhead with exhaust gas recirculation (Figure 2- 2). With this design, we can produce desired gradients of gas impingement or deposition – or uniformity – across the wafer surface. Initial feasibility of the programmable CVD concept was demonstrated in prototype reactors.^{48, 49} The programmable CVD system has two chambers: the load lock chamber and reaction chamber (reactor), both made of ultrahigh vacuum grade stainless steel. The current

programmable CVD reactor design includes a three-segment showerhead, recirculated exhaust gas flow through the showerhead, and a dynamic multiplexed sampling system for multi-point real time process monitoring.⁵⁰ The present three-segment design of the CVD showerhead is intended to prove feasibility, validate models, and demonstrate control. Manufacturing implementation will require scaling to more segments, higher spatial fidelity and control. We have developed a process sensing and control system for the novel SP-CVD equipment, along with dynamic software models to guide the equipment design, the corresponding process control, and the rapid optimization of materials deposited. The sensor design employs multiplexed mass spec sensing in the SP-CVD system, extending such real-time sensing and metrology distinctly beyond the state of art.

A front view of the mechanical design of the programmable CVD reactor is shown in Figure 2- 3. There are three segments in the reaction chamber, each of which has two gas feed tubes and one mass spec sampling tube. Based on previous experimental and simulation work, we set the distance (h) between the wafer surface and the gas feed tube outlet as 2.25 inches.^{49, 13} A linear motion device enables adjustment of gap (z) between the bottom of the showerhead and the wafer, thereby controlling the inter segment diffusion. A substrate heater is employed to heat the wafer to a temperature of 350°C to 400°C during the deposition. Figure 2- 4 shows the picture of the real SP-CVD system.

There are two mechanisms of inter-segment gas mixing in the SP-CVD. One mechanism is convective gas mixing; another mechanism is mixing by gas diffusion. The segmented showerhead design minimizes inter-segment convective gas mixing

by drawing exhaust gas back up through the showerhead segment. This is very critical for programmable CVD system because the segments separate the process into three decoupled zone. However, inter-segment gas diffusion still exists in the SP-CVD reactor. As shown in Figure 2- 5, there are two zones where inter-segment gas diffusion takes place in the reactor: (1) Inter-segment gas mixing across the wafer (ISM-wafer) in the region between the wafer and the segment bottom; (2) Back diffusion (ISM-BD) of gases from one segment through the common exhaust port and back down into an adjacent segment. Inter-segment gas diffusion is not desirable in the deposition process since it disturbs the process in the neighbor segment.

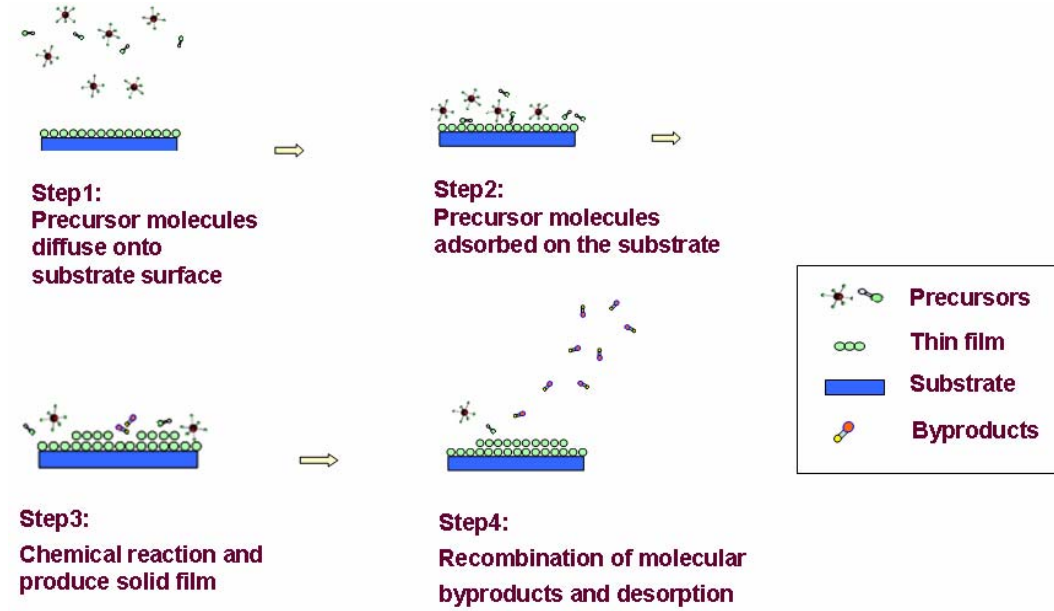


Figure 2- 1 Chemical vapor deposition (CVD) reaction

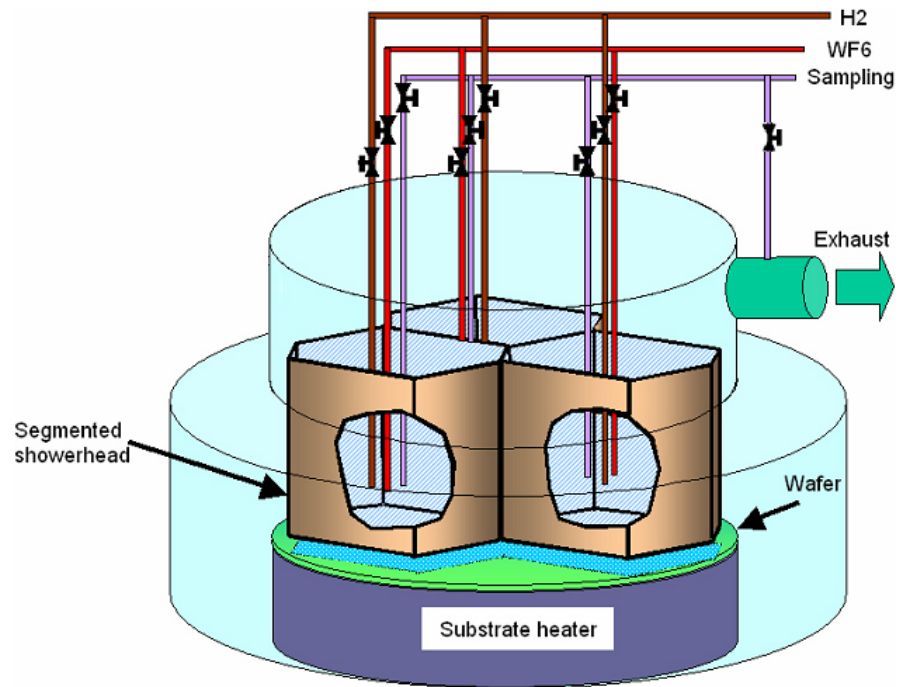


Figure 2- 2 Programmable CVD reactor design

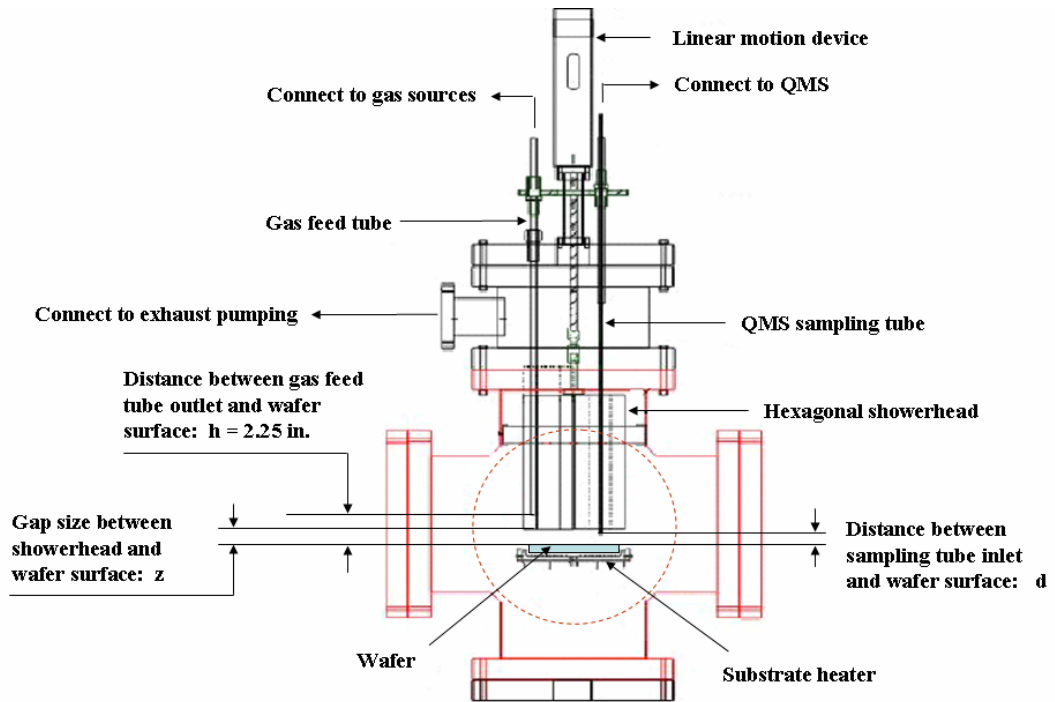


Figure 2- 3 Front view of programmable CVD chamber mechanical design.

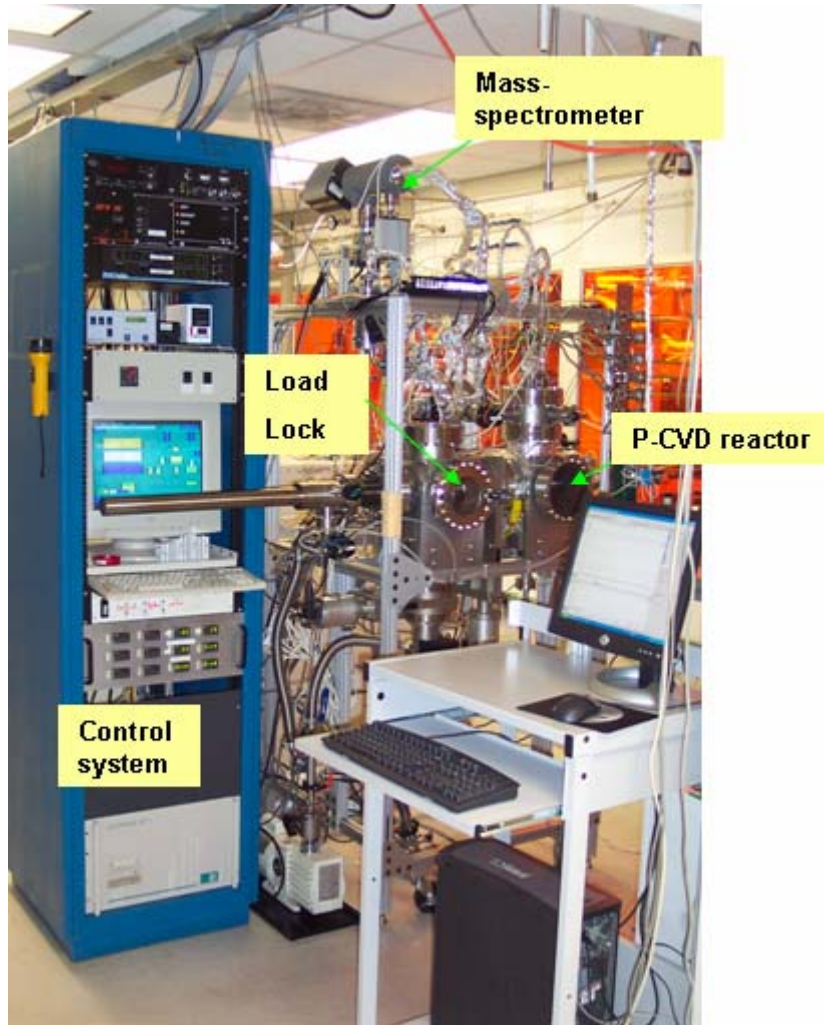


Figure 2- 4 Spatially programmable chemical vapor deposition (SP-CVD) system.

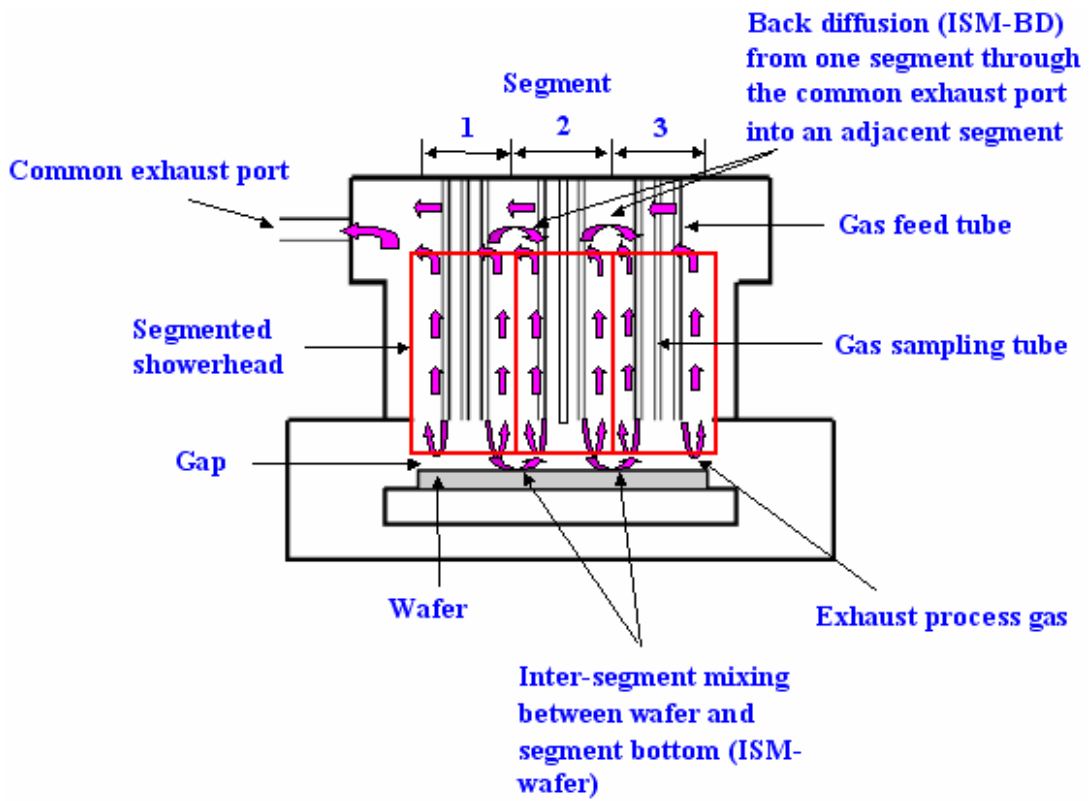


Figure 2- 5 Gas flow in the SP-CVD reactor.

Chapter 3: Design and implementation of multiplexed mass spec sensing in SP-CVD

3.1 Real time APC with in situ sensing for process metrology and process control

Real time metrologies will drive course correction to keep the process stable. In real-time APC, *in situ* sensors are employed to continuously sense and calculate process data, adjust process parameters and keep the process at the desirable status. Both long term and short term process drifts can be compensated by real-time APC.¹ Moreover, in the fault management, real-time *in situ* sensing is more effective to detect problems from process/system and further initiate corrective actions. Mass spec is an ideal *in situ* sensor because it does not come in contact with the wafer or change the CVD process, and yet, it provides sensitive measurements of gas compositions and therefore, helps obtain real-time information about the process.

3.2 Multi-point mass spec sensing

In order to study the gas flow behavior within the three segments, multi-point mass spec sensing has been introduced in the SP-CVD system as indicated by the QMS sampling tube in Figure 2- 3 and shown by the photo in Figure 3- 1. There are nine tubes in the segmented showerhead: tubes A1, A2 and A3 are the QMS sampling tubes; tubes B1, C1, B2, C2, B3, C3 are gas feed tubes. We changed the vertical position (d) of the sampling tubes in order to study the gas distribution within a segment. We used inert gases, which are sufficient for this study, in order to minimize any safety concerns during movement of the tubes on O-ring seals.

3.3 Pressure transduction strategy for gas sampling

3.3.1 Mass spec and pressure reduction requirements

The mass spec system, an Inficon Transpector™, consists of a closed ion source (CIS), a quadrupole mass filter and an ion detector mounted in a chamber. At the outside of the mass spec chamber, an electronic module is used to control the operation of the mass spec and transfer the monitor data to a computer through an RS-232 interface. A BAG100-S Bayard Alpert Gauge is attached to the mass spec chamber to check its pressure. A turbomolecular (turbo) pump is integrated with the mass spec chamber to maintain a high vacuum (10^{-8} torr). In order to dilute corrosive gas concentrations, the pump is purged with 10 sccm of N₂ gas.

The mass spec separates the different gas ions according to their *mass-to-charge ratio* (m/z), distinguishing m/z by their different paths in electric and RF fields. In order to determine m/z , ions pass through the spectrometer system without collisions with other molecules or ions, meaning the QMS must maintain molecular flow, where approximately $P < 10^{-5}$ Torr. Since the CVD processes of interest are in the range of 100 mTorr to 10 Torr, a pressure reduction method is needed which effectively samples CVD gas flows into the QMS system, as is seen in the literature.^{19, 51}

3.3.2 Simulation model for pressure reduction design

We define the time it takes the process gases from the wafer surface to reach the mass spec sensor as the gas transfer time. If the gas transfer time is too long, we can only monitor the process, which has happened in the past. Thus, short gas transfer

time and low pressure in the mass spec chamber are the key factors to achieve multiplexed real-time chemical sensing. Prior work shows that a workable method of sampling from a CVD process or plasma etching process chamber is to use a multi-stage pressure reduction scheme.^{19, 52} A small amount of gas is drawn into a sampling tube through a small orifice by a differential pumping system, which was attached to the mass spec chamber. The schematic of the pressure reduction design in the mass spec sampling system is shown in Figure 3- 2.

The diameter of orifice 1 is the key parameter in determining the gas transfer time of the sampling system and the pressure in the QMS. It is necessary to perform simulations in order to calculate the size of the orifice; thus a simulation modeling was established as follows before settling on a final design.⁵³ The gas flow before orifice 1 is in the viscous flow regime and the gas flow after orifice 2 is in the molecular flow regime.

$$Q = S * P_3$$

$$C_{Eff} = \frac{1}{\frac{1}{C_{tube}} + \frac{1}{C_{CIS}}}$$

$$C_{tube} = 3.81 * (T / M)^{1/2} (D^3 / L)$$

$$P_2 = P_3 + \frac{Q}{C_{Eff}}$$

$$C_{orifice1} = \frac{Q}{P_1 - P_2}$$

Where,

Q: Throughput of QMS pumping system;

S: Turbo pump pumping speed;

P₃: Operational pressure of QMS pumping system;

C_{tube}: Sampling tube conductance;

C_{CIS}: Closed ion source conductance;

T: Gas temperature;

M: Molecular weight;

D: Inside diameter of sampling tube;

L: Length of sampling tube;

P₁: Process pressure;

P₂: Pressure inside orifice 1.

In our system, the reactor pressure P₁ is 1 Torr. We set the mass spec chamber pressure P₃ at 10⁻⁵ Torr. The conductance of a closed ion source is around 0.7 L/sec,³¹ turbo pump pumping speed S is 30 L/sec and the length of ¼ inch sampling tube is 62 inches. As a result, the diameter of the orifice 1 can be calculated by:

$$A = \frac{C_{orifice}}{11.6 * k}$$

$$d = \sqrt{\frac{A}{\pi}} * 2$$

Where,

A: Orifice area;

k: Conversion factor from air to other gas.

Since multiplexed sampling in SP-CVD is a complex dynamic process, we built the modeling and simulation by VisSim[®] software program. Calculation results based on the above modeling show the diameter of orifice 1 is 35 μ m.

3.4 Multiplexed gas sampling system design

3.4.1 Using the mass spec for sampling of the three segments

The unique design of the multiplexed mass spec sampling system gives us the opportunity of using one mass spec to multiplex the sampling of gases from the three segments. Our current design of an SP-CVD reactor is only a prototype reactor with three segments and is used to prove the SP-CVD concept. However, in the future, if SP-CVD is applied by the manufacturing industry, more than three segments may be used and multiplexed mass spec sampling will become even more beneficial.

A detailed view of the mass spec multiplexed sampling system is shown in Figure 3- 3. Each sampling tube employs an orifice (orifice 1) at its entrance near the wafer in order to sample gas. However, when another segment is being sampled, gas between orifice 1 and the QMS must be quickly removed, otherwise, it generates a high background QMS signal. Therefore, a bypass line is used to accomplish this for each segment. All three bypass lines are connected together with a differential pumping system, which consists of a turbo molecular pump and a diaphragm pump. Valve 1, valve 2 and valve 3 are the valves connected between each sampling tube to the mass spec chamber; valve 1' , valve 2' and valve 3' are the valves connected between each sampling tube to the bypass line.

When segment-X (X=1, 2 or 3) is not monitored, sampling tube-X is in an idle state, most of the gas, which comes from the programmable CVD reactor through the orifice, is removed by the bypass line pumping system. During observation of segment-X, the valve to the bypass line is closed and all gases flow into the ion source region of the mass spec for analysis.

Operation of these control valves is summarized in Table 3- 1. During the process, if the mass spec is monitoring segment-1, then valve 1 opens, while its bypass line is closed. During this time, the other two segments' sampling tubes to the QMS are closed and their bypass lines are opened.

The mass spec pressure is compared in the two settings of valve 1' during the monitoring of segment-1: (1) If valve 1' is closed, the pressure in the mass spec chamber is approximately 10^{-6} Torr. (2) If valve 1' opens, the pressure in the mass spec chamber is approximately 10^{-5} Torr. The low-pressure valve setting was chosen in order to prevent the ion source of the mass spec from being damaged. Therefore, when segment-X (X=1,2, or 3), is monitored, valve X' is closed. When segment-1 is monitored, valve 2 and valve 3 are closed while valve 2' and valve 3' are opened to maintain low pressure in the sampling tubes of segment-2 and segment-3. To switch monitoring from segment-1 to segment-2, valve 1 and valve 2' are closed and valve 1' and valve 2 are opened. Because most of the sampled gas in the sampling tube of segment-2 is pumped out through the bypass line, only a small fraction of the sampled gas flows into the mass spec chamber for analysis. Test results reveal that the gas transfer time from the SP-CVD reactor to the mass spec is less than 1 seconds and the pressure in the mass spec chamber is as low as 10^{-6} Torr.

3.4.2 Using the mass spec for process fault detection and contamination control

In addition to monitoring gas composition in each segment, the mass spec sampling system also was designed for process fault detection and monitoring equipment contamination. As shown in Figure 3- 3 (part 2), a 35 μ m orifice sampling tube coupled with a bypass line is connected with the common exhaust area to sample the gas from all three segments in the programmable CVD reactor. For process fault detection during programmable CVD process, we open valve 4' and close valve 4. The gas will go through the 35 μ m orifice and flow into the mass spec chamber. To monitor chamber contamination level, we open valve 4 and close valve 4' . The gas in the reactor will flow into mass spec through the bypass line. However, this can only be conducted when the chamber pressure is lower than 10⁻⁵ Torr, because there is no orifice connected in the bypass line.

Previous experiments indicate that the purity of the precursor gas is a critical factor for the quality of CVD thin film. Water, oxygen, nitrogen and other contaminants can accumulate on the inside surface of the gas delivery system and decrease the purity of the precursor. As shown in Figure 3- 3 (part 3), the mass spec inlet system also includes a 2 μ m orifice tube and a bypass line connected with each gas delivery line. This enables checking the purity of precursor directly from cylinder (in Figure 3- 3 part 3, the valve in the bypass line is closed and the precursor goes through 2 μ m orifice) and the contaminant level in the gas delivery system (in Figure 3- 3 part 3, the valve in the bypass line is opened) by the same mass spec as we used for the programmable CVD process monitoring.

3.5 Mass spec signal integration

As explained in Chapter 3.4.1, one mass spec was used to monitor the process within three segments and the monitoring was switched between segments every 20 seconds. The mass spec signal shown from the TWare 32 is a mixed signal from three segments: the signal from the 1st 20 sec is the monitoring signal in segment 1, the signal from the 2nd 20 sec is the monitoring signal in segment 2, the signal from 3rd 20 sec is the monitoring signal in segment 3, etc. Therefore, SP-CVD sensing virtual instrument (VI) was developed to collect the mass spec signal from process, to separate the mixed mass spec signal into three groups and to integrate the mass spec signal for each segment. The SP-CVD sensing virtual instrument (VI) is based on the National Instrument's LabVIEW[®] platform. By using the Dynamic Data Exchange (DDE) protocol, SP-CVD sensing VI can collect and analyze the mass spec signal data from mass spec software package TWare 32 in real-time. DDE is a Microsoft protocol that allows for communication channels to be established between multiple software programs running on the same computer system (or network). TWare 32 acts as the server and provides data for the SP-CVD sensing VI client. The DDE establishes communication channel between TWare 32 and SP-CVD sensing VI client so that they can communicate with each other.

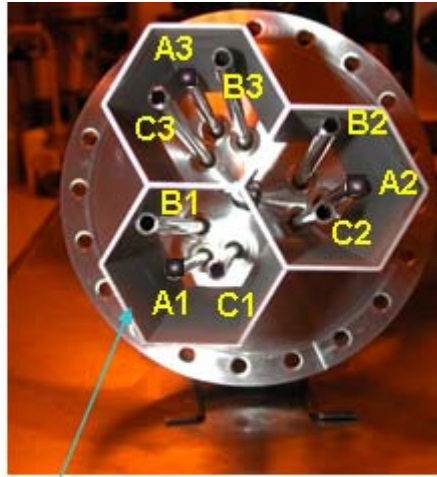
Figure 3- 4 explains the concept of data separation. Different color bar represents the mass spec signal from a different segment. The SP-CVD sensing VI collected the mass spec signal through DDE and separates them into three groups. The data from the first 20 seconds, which means the mass spec monitoring signal from segment 1 was put into group 1; the data from the second 20 seconds was put

into group 2; and the data from the third 30 seconds was put into group 3. Then the SP-CVD sensing VI repeated this data separation process. Simultaneously, SP-CVD sensing VI performed signal integration for each segment in real time. Figure 3- 5 is a snapshot of the front panel of SP-CVD mass spec sensing VI. It shows the separated mass spec signal and the integrated mass spec signal from each segment. In Chapter 2.2, W CVD reaction [2] shows HF is the byproduct gas from H₂ reduction of WF₆. Previous study from our group has proved that by monitoring the amount of HF gas, we can predict how much W film has been deposit on the wafer. This approach was used in this research to develop a mass spec sensor based film thickness metrology. The detailed metrology development and process control by using integrated mass spec signal will be described in Chapter 5 and Chapter 6.

Table 3- 1 Valve operation of the mass spec sampling system

	Segment 1 valves		Segment 2 valves		Segment 3 valves	
	Sampling tube	Bypass line	Sampling tube	Bypass line	Sampling tube	Bypass line
Sample segment 1	O	X	X	O	X	O
Sample segment 2	X	O	O	X	X	O
Sample segment 3	X	O	X	O	O	X

O: open X: closed



Hexagonal segmented showerhead

Figure 3- 1 Bottom view of the programmable CVD showerhead

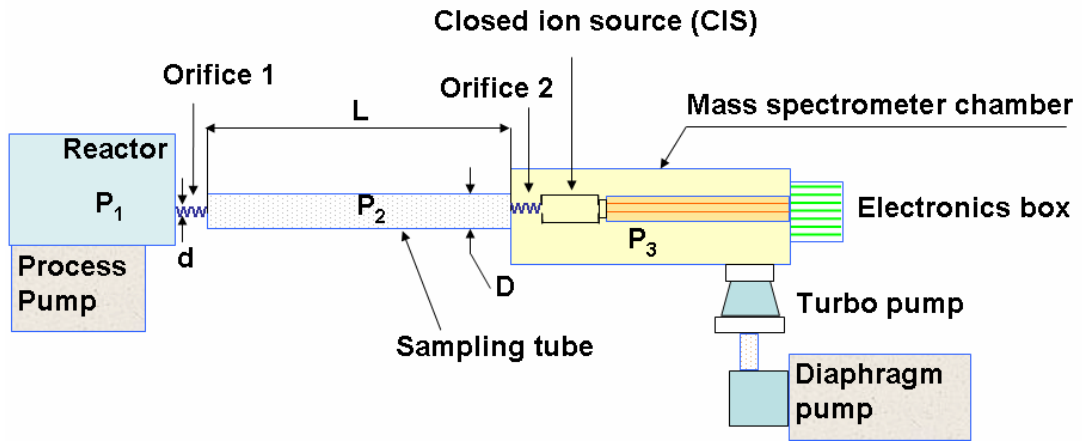


Figure 3- 2 Schematic of pressure reduction in the mass spec sampling system.

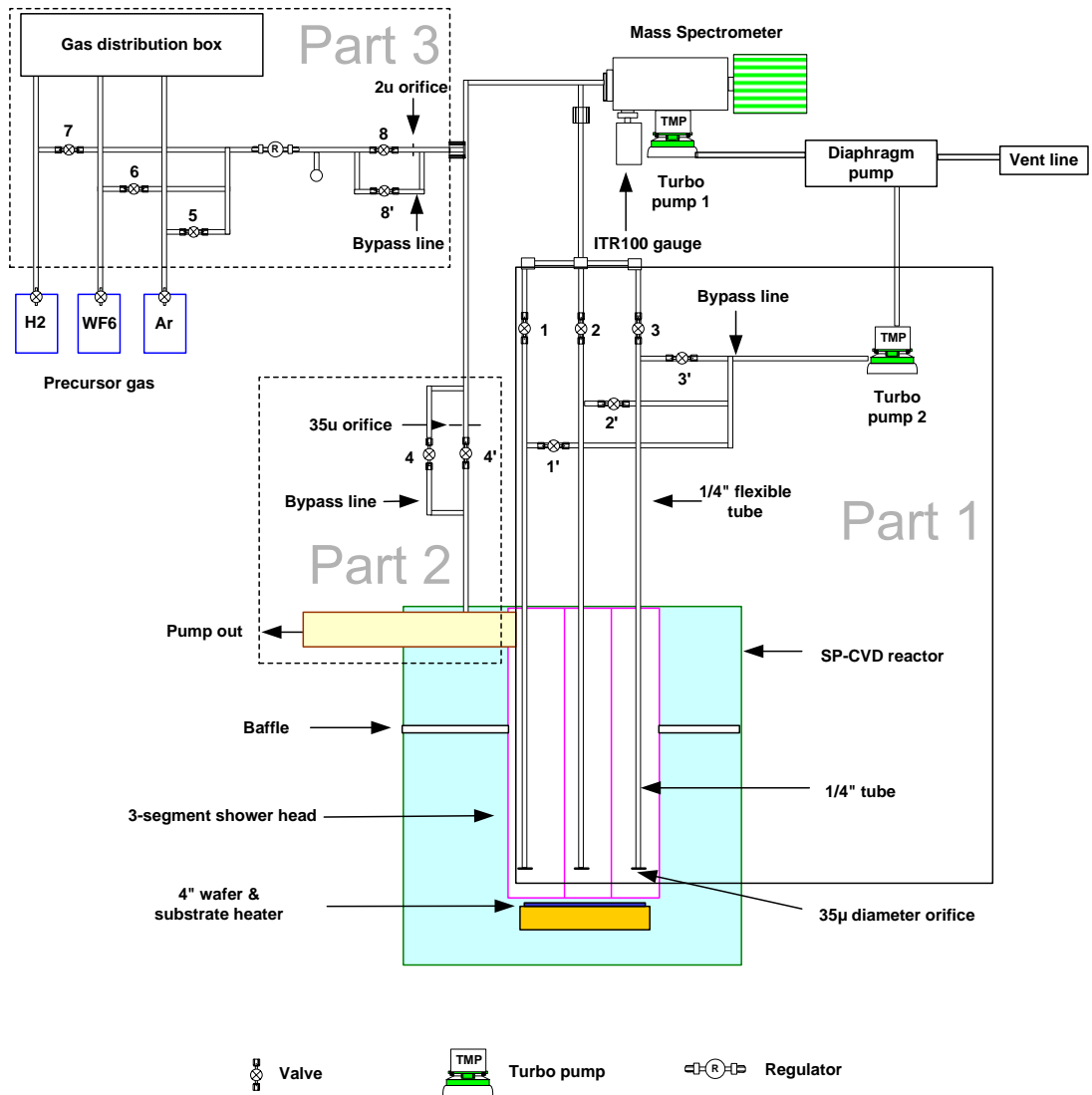


Figure 3- 3 Schematic diagram of multiplexed mass spec sampling system.

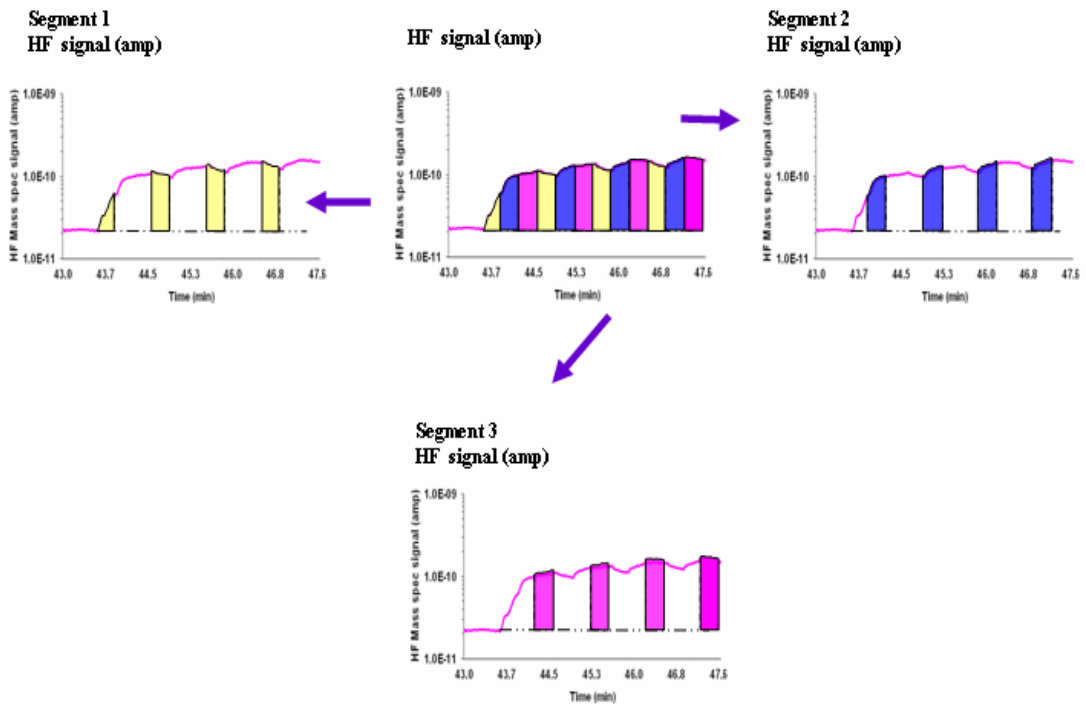


Figure 3- 4 Mass spec signal separation.

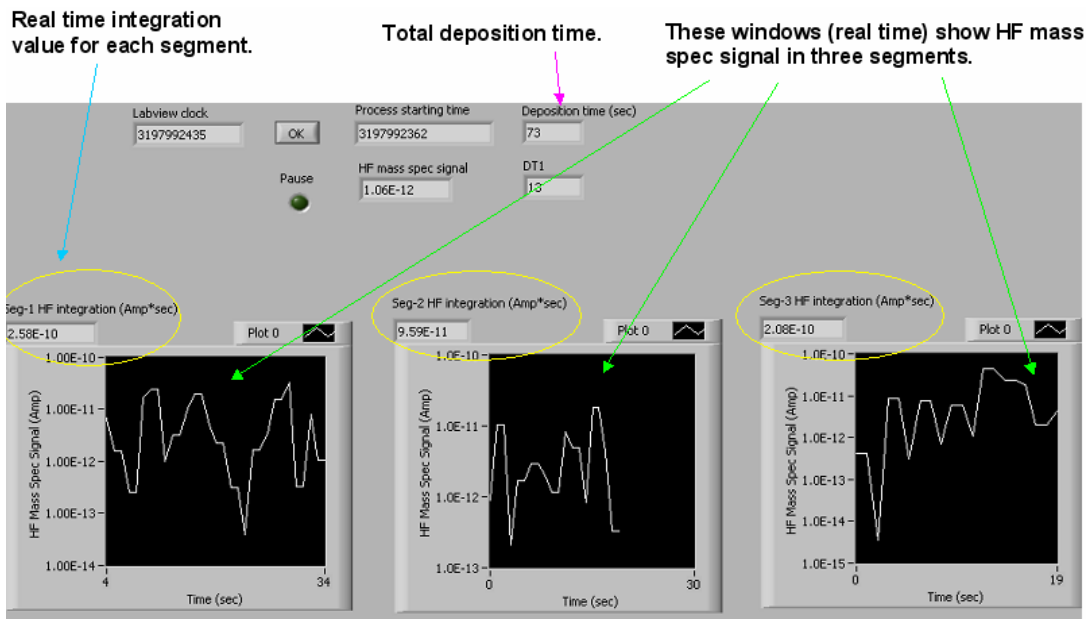


Figure 3- 5 SP-CVD mass spec sensing VI front panel.

Chapter 4: Gas distribution and gas transportation mechanisms in SP-CVD reactor

4.1 Mechanisms of inter-segment gas diffusion

One unique design feature of the programmable CVD system is the process gas exhausting through a common exhaust port at the top of showerhead.^{46,50} As mentioned in Chapter 2, there are two types of inter-segment gas mixing in SP-CVD reactor (as shown in Figure 4- 1): (1) inter-segment mixing across the wafer (ISM-wafer) in the region between the wafer and the segment bottom; (2) back diffusion (ISM-BD) of gases from one segment through the common exhaust port and back down into an adjacent segment. The intra segment gas distribution at the different vertical positions is affected by both of these two types of gas diffusion. The distance between the segment and the wafer surface is particularly critical in that it controls the effect of ISM-wafer at the wafer surface. A smaller gap is desirable for greater spatial control and a larger gap is desirable for smoother gradients across the wafer.

Mass spec has been used to experimentally validate the mechanisms of gas diffusion. Table 4- 1 shows the gas flow rates in three segments. In Experiment 1, 60sccm of Ar gas was injected into segment-1 and segment-2; meanwhile, 60sccm of N₂ gas was injected into segment-3. Figure 4- 2(a) shows Ar and N₂ mass spec signals in segment-2 and segment-3. Ideally, if gas diffusion is not considered, the mass spec signal will be like the “ideal signal” shown in Figure 4- 2(a). However, experimentally, the two types of gas diffusion have strong effects on the gas

distribution in each segment. When the gap size between the wafer surface and the bottom of the segmented showerhead was set at 32mm, Ar and N₂ gases were mixed above the wafer surface. Therefore, this gap size at the wafer surface promotes substantial ISM-wafer in addition to ISM-BD. In the next step, the segmented showerhead was lowered from 32mm to 1mm. As the position of the segmented showerhead was lowered, the effect of ISM-wafer was reduced. The mass spec signal showed that, in segment-2, the Ar signal increased while the N₂ signal decreased; in segment-3, the N₂ signal increased while the Ar signal decreased. Since only Ar was flown in segment 2 and only N₂ was flown in segment 3, a smaller gap makes their concentrations purer in the respective segments.

A second experiment (Experiment 2) was performed in order to study the relationship between the gas flow rates and inter segment gas diffusion. In Experiment 2, the gas flow rates in each segment were reduced in half (Table 4- 1). Similarly, a QMS signal trend was obtained in Experiment 2 (Figure 4- 2(b)). However, the difference between the Ar signal and the N₂ signal has decreased from A (3.06×10^{-10} AMP) to B (1.85×10^{-10} AMP). With a smaller gap, the gas purity in each segment is subsequently increased; however, the gas in Experiment 2 is not as pure as that in Experiment 1 since there is more ISM-wafer effect at lower gas flows.

From this experiment, we validated that: (1) The showerhead segment can separate the different CVD processes in one programmable CVD reactor. (2) High gas feeding rates will prevent gas diffusion (both ISM-wafer and ISM-BD) from other segments. These results are consistent with previous simulation models.⁵⁰

4.2 Quantify the contribution of signal from ISM-wafer and ISM-BD

A series of experiments were conducted to quantify the contribution of the signal from the gas diffusion through the gap between the wafer and the showerhead (ISM-wafer) and from the common exhaust area (ISM-BD). In Experiment 3 (shown in Figure 4- 3), segment-3 was monitored to measure the H₂ signal, which was only contributed by gas diffusion from segment-2. 30 sccm of Ar and 30 sccm of H₂ were flowed into segment-2, 60 sccm of Ar was flowed into segment-1 and segment-3 respectively. First, we set a 0mm gap (no gap) between the segmented showerhead and the wafer surface. Then, we increased the gap size from 0mm to 1mm, 2mm, and 3mm. The mass spec monitored segment-3 and the resulting H₂ signal is shown in Figure 4- 3, Experiment 3. H₂ was not flown through segment-3 for a gap size of 0mm, therefore, the resulting H₂ signal in segment-3 is due to the H₂ ISM-wafer from segment-2. Furthermore, the contribution of the signal from the gas diffused through the gap (ISM-wafer) can be calculated by taking the difference between H₂ signals from an Xmm (X=1, 2, or 3) gap size and the 0mm gap size.

In Experiment 4 (Figure 4- 3), segment-3 was still monitored, however the recipe in segment-1 was changed to 30 sccm of Ar plus 30 sccm of H₂. The measured H₂ signal in segment-3 had contributions from other segments due to gas diffusion. By comparing the H₂ signal taken from the 0mm gap size in Experiment 3 and Experiment 4, it was found that the H₂ signal from Experiment 4 (2.26×10^{-9} amp) almost doubled the H₂ signal from Experiment 3 (1.32×10^{-9} amp) in segment-3. This is because in Experiment 3, only segment-2 contributed H₂ to segment-3 from the common exhaust port; however, in Experiment 4, both segment-1 and segment-2

could contribute H₂ to segment-3 from the common exhaust port. Therefore, the H₂ signal is almost doubled, as in Experiment 3.

4.3 Concentration profiles along vertical showerhead segments

We have used mass spec to validate and quantify two types of gas diffusion in SP-CVD processes. In order to understand how these two types of inter-segment gas mixing affect the gas distribution in each segment, the mass spec was further applied to monitor the gas distribution at the different vertical positions within one segment. Before the SP-CVD system was built, Dr. Adomaitis' group developed a simulation-based design to model the SP-CVD.⁵⁰ The mass spec was used to evaluate this modeling.

A movable mass spec sampling method has been employed by Kastenmeier et al. and Xi Li et al. to monitor chemical processes.⁵⁴ We applied this approach to understand the gas composition profile in one segment.

In this evaluation experiment, the gap between the showerhead and the wafer surface was fixed at 1mm, with 60 sccm of Ar gas flowed into both segment-1 and segment-3; a mixture of 30 sccm of Ar and 30 sccm of H₂ was flowed into segment-2. The reaction chamber pressure was kept at 1 Torr. Initially, the distance between the wafer surface to the bottom of the sampling tube and the bottom of the feeding tube were set at 0.5 inches and 2.25 inches respectively. Figure 4- 4 (a) presents the Ar and H₂ gas composition profiles at the different height positions in segment-2. The Ar signal is much higher than the H₂ signal even when the same amount of Ar and H₂ was flowed through segment-2. The Ar gas came from two main sources: (1) Ar gas

was introduced through the gas feed tube; (2) Ar gas diffused from the other segments (ISM-wafer + ISM-BD).

The position of the bottom of the sampling tube to the wafer surface was moved up from 0.5 inches to 4.5 inches. As shown in Figure 4- 4 (a), before the outlet position of gas feed tube (2.25 inches above the wafer surface), the Ar signal decreased as the sampling tube was moved up. As explained in Figure 4- 4 (b), the higher Ar signal at low positions was caused by Ar diffusing from other two segments to segment 2 (ISM-wafer dominates at low positions). As the sampling tube reached 2.5 inches, which is a little higher than the outlet of the gas feed tube position, the Ar signal reached its lowest value. Thereafter, the sampling tube continued to be lifted; however, the Ar signal started to increase. This signal increasing was due to Ar in the other segments back diffusing to segment-2 from the top exhaust area (ISM-BD dominates at high positions). Compared to the Ar signal, the profile of the H₂ signal in segment 2 has the opposite trend. The highest value of the H₂ signal was obtained around the outlet position of gas feed tube. H₂ showed lower signal at both higher position and lower position of the segment.

The mass spec signal is a current signal related to the partial pressure of the measured gas; however, for the purpose of these experiments the current signal was converted into the gas compositions mole fractions. Figure 4- 5 compares the converted gas concentration profile with the gas concentration profile taken from the simulation modeling.⁴⁹ It is obvious to see that both of the experimental results and the simulation results indicate the same trend of the gas concentration profile at the different vertical positions in segment-2.

In addition to the experiment of different gas flow into different segment, we also conducted the experiment with feeding the same gas into all segments and evaluated the gas composition profile at the different height position within one segment. As the result shown in Figure 4- 6, both of H₂ signal and Ar signal did not change as sampling tube position moved up. This gas composition profile is different with the profile shown in Figure 4- 4. Since all the segments were fed with the same gas (30sccm Ar + 30sccm H₂), there was no driving force for diffusion between segments. So the gas composition is same at all the positions along the vertical direction of the segment.

Table 4- 1 Gas flow rates in three segments.

Experiment 1

Segment #	1	2	3
Ar flow rate (sccm)	60	60	0
N₂ flow rate (sccm)	0	0	60

Experiment 2

Segment #	1	2	3
Ar flow rate (sccm)	30	30	0
N₂ flow rate (sccm)	0	0	30

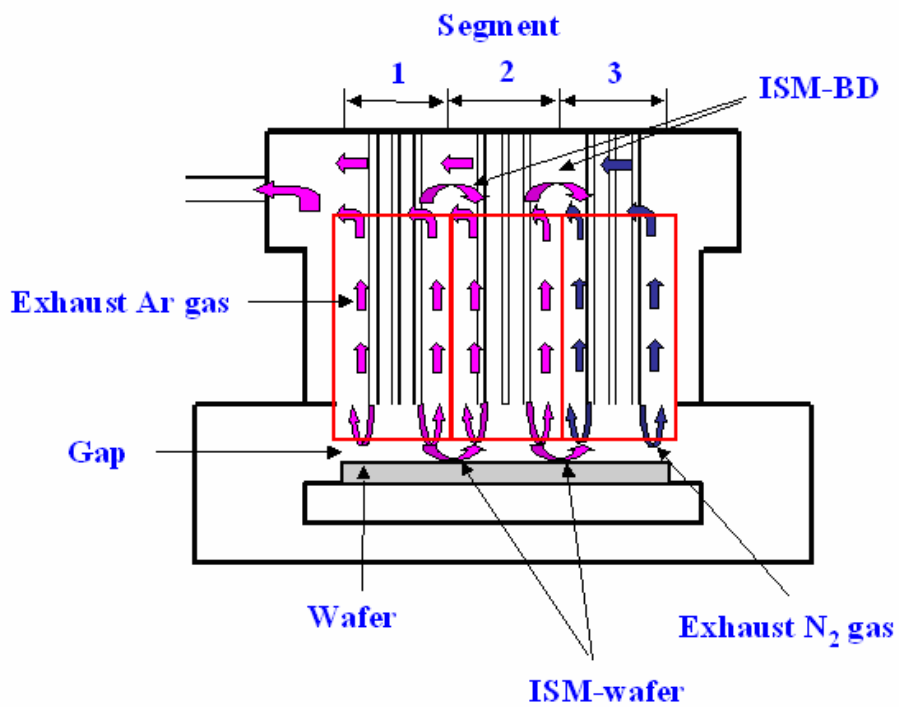


Figure 4- 1 Two types of inter-segment gas mixing

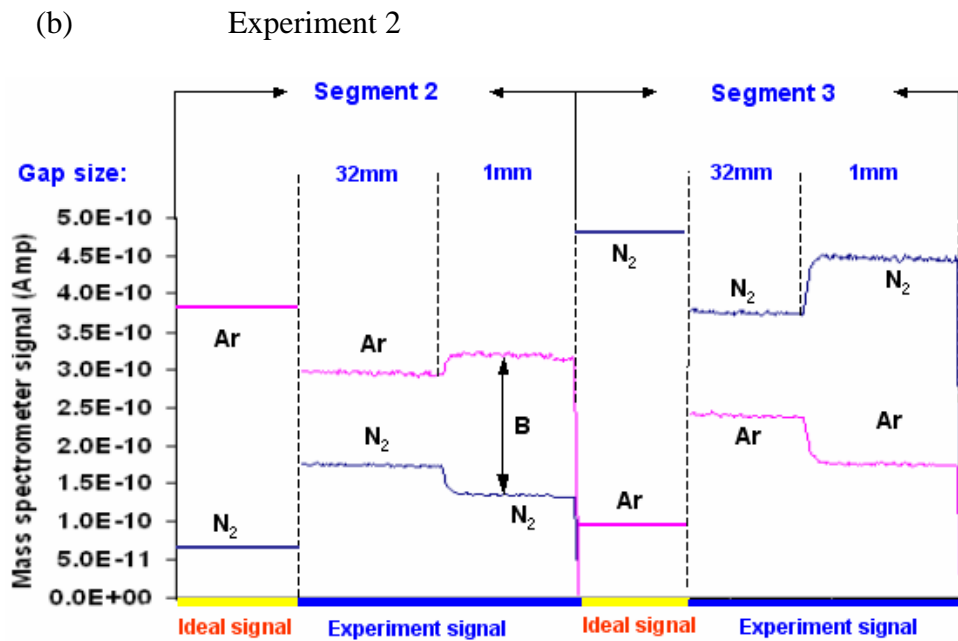
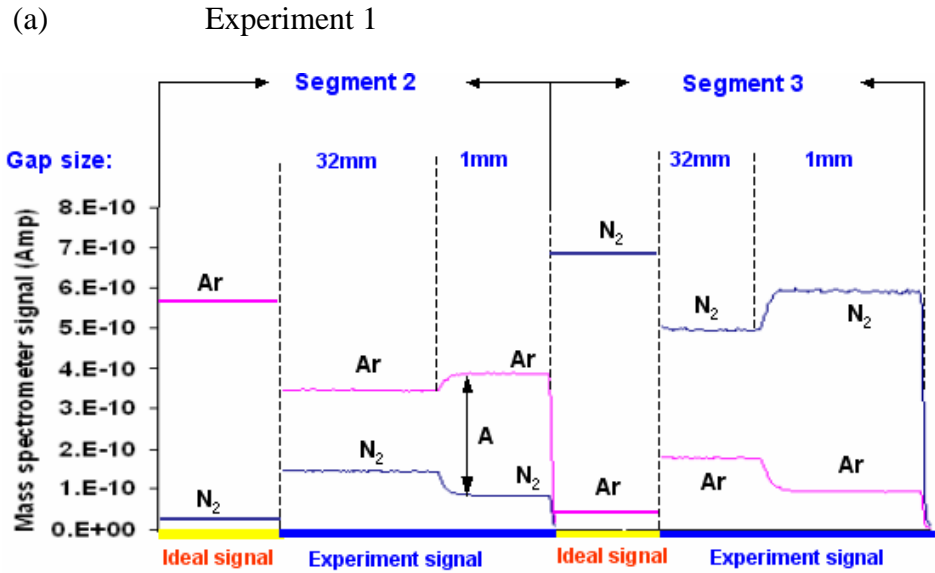
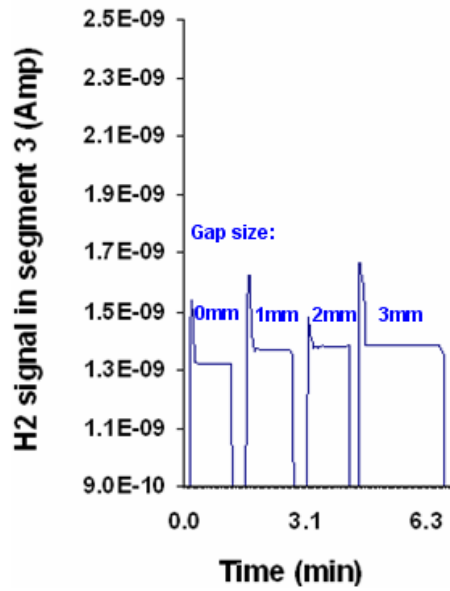


Figure 4-2 QMS signal validates the recirculated gas flow in programmable CVD showerhead.

Experiment 3

Segment #	1	2	3
Ar (sccm)	60	30	60
H ₂ (sccm)	0	30	0



Experiment 4

Segment #	1	2	3
Ar (sccm)	30	30	60
H ₂ (sccm)	30	30	0

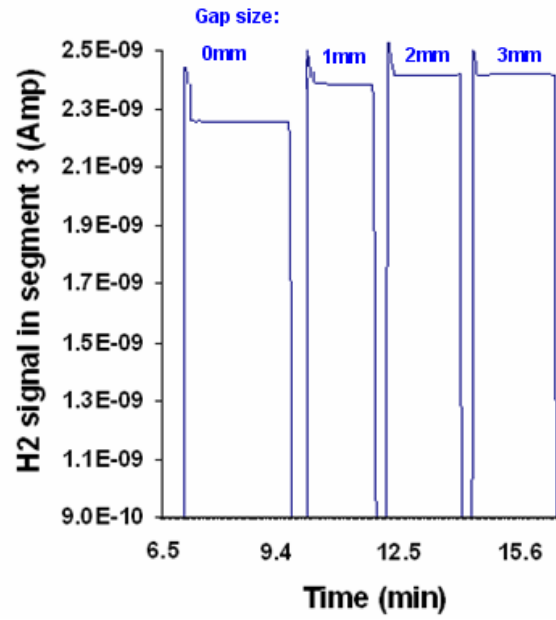


Figure 4- 3 Quantify contribution of H₂ signal from inter-segment gas diffusion

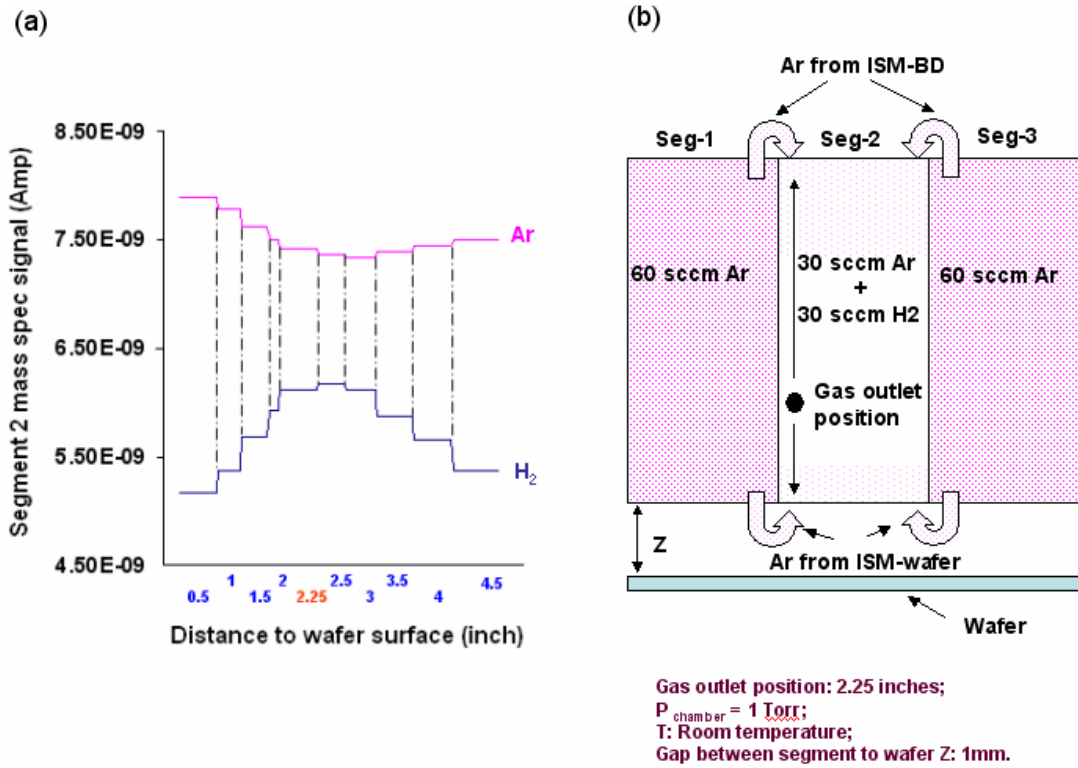


Figure 4- 4 Gas composition at the different positions in segment-2 with a 1mm gap size between the showerhead and the wafer surface.

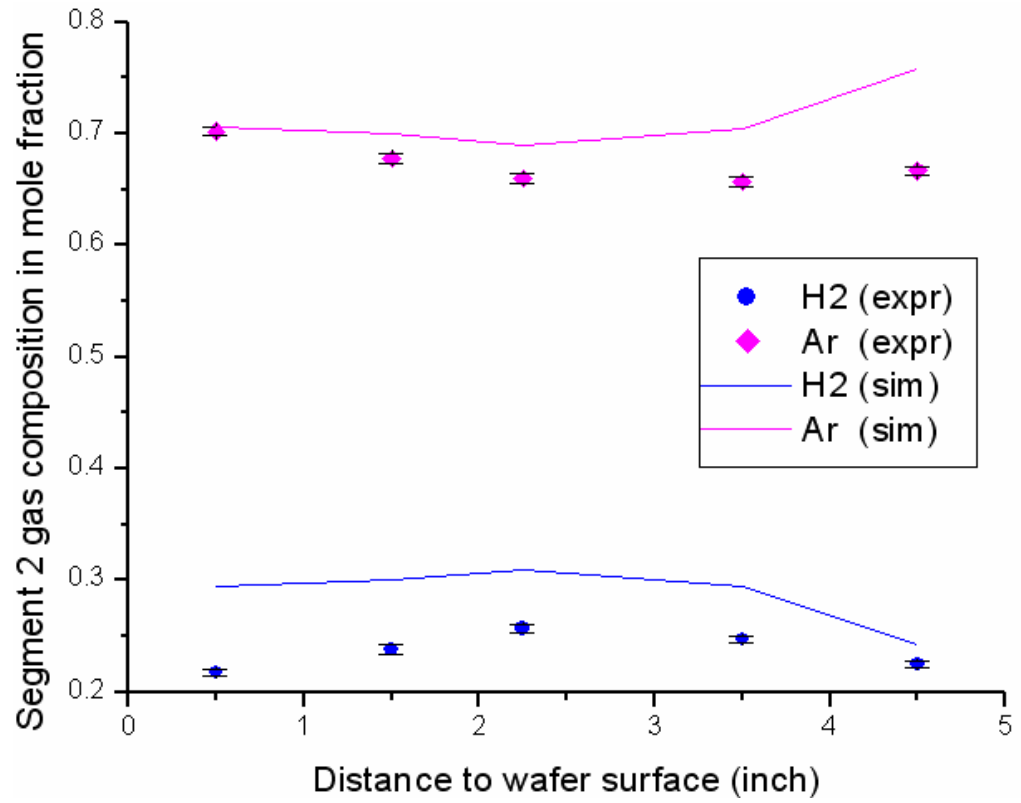


Figure 4- 5 Gas composition in mole fraction in segment-2 (experimental result and simulation data), the standard deviation of experimental data is within 0.3%~0.4%.

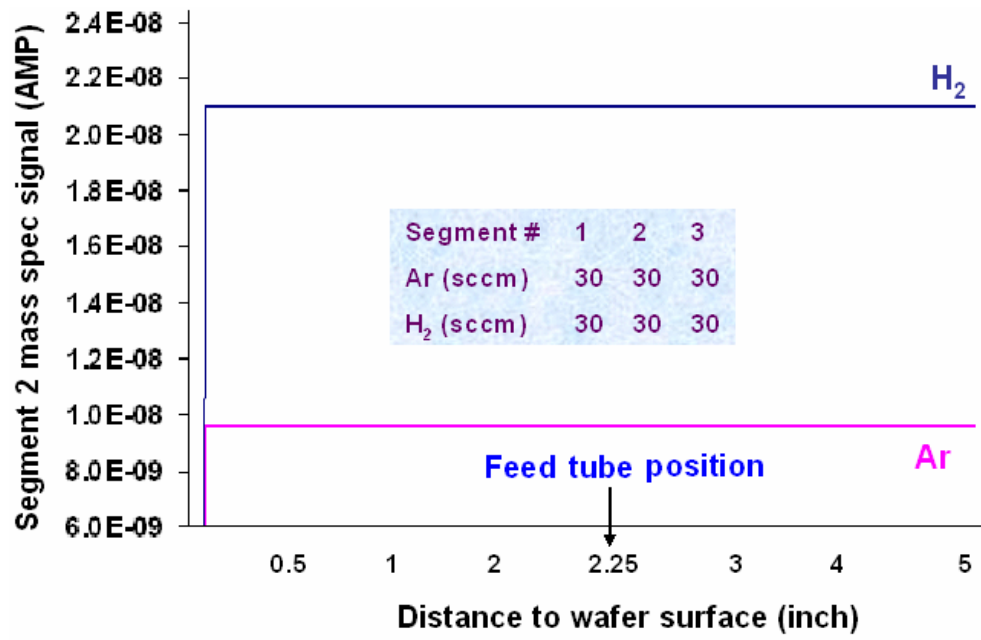


Figure 4- 6 Ar and H₂ mass spec signal as a function of position in segment-2 when feeding the same gas in three segments.

Chapter 5: SP-CVD experimental procedure

5.1 Methodology

5.1.1 Equipment conditioning

In order to achieve good deposition results on the wafer, reducing the contamination level in the CVD system is critical. It is known that WF_6 , HF and H_2O condense on the inside surface of SP-CVD system. Therefore if H_2O is not reduced, it will react with WF_6 and form HF during the H_2 reduction of WF_6 experiment (reaction [3]).



When the mass spec senses the HF signal, it cannot distinguish the HF signal between that obtained from the H_2 reduction of WF_6 (reaction [2]) and that obtained from the reaction of H_2O with WF_6 (reaction [3]). It will be explained why the HF mass spec signal was chosen as the metrology signal in Chapter 5.2.3. The HF signal from reaction [3] can affect the accuracy of the mass spec metrology. Hence, before the deposition experiment, the SP-CVD reactor, gas delivery system, and mass spec sampling system were baked at 150 ° C for 3-4 days. After baking, the mass spec showed that the H_2O levels within the SP-CVD reactor had decreased from 10^{-10} AMP to $10^{-14} \sim 10^{-13}$ AMP.

Before the deposition process, a mixture of WF_6 and H_2 gases were flown into the SP-CVD system for equipment conditioning. A dummy wafer was used during this conditioning process. The parameter settings (pressure/temperature/process time) were the same settings used during the real deposition process. Meanwhile, the mass spec also conducted the same monitoring procedure as conducted during the real deposition experiment. There are three reasons to perform equipment conditioning: (1) Reduce water vapor residual in the reactor and gas delivery system by H_2O reduction of WF_6 . (2) Passivate the reactor wall by saturating the reactant and byproduct gases in the reactor. (3) Allow the mass spec signal to reach a stable status after continuously running for 2~3 hours.⁵⁵ After this conditioning sequence, the mass spec signal was checked. If the deposition from two consecutive conditioning wafers showed the same value of time integration of the HF mass spec signal, it was determined that the reactant and byproduct gases saturated the inside walls of the SP-CVD reactor. The conditioning procedure for these experiments usually take about 3 hours.

5.1.2 Experimental procedure

The W CVD process was carried out in the SP-CVD reactor by the following sequence of steps: (1) a 4 inch Si wafer was cleaned by a 10% HF solution in order to remove the surface layer of SiO_2 (five minutes); (2) the Si wafer was dried by compressed N_2 ; (3) the wafer was then manually loaded into the load lock chamber (this was done in order to keep the SP-CVD reactor clean); (4) next, the wafer was transferred into the SP-CVD reactor when the pressure in the load lock chamber reached a level below 10^{-4} torr. (5) The process pressure was kept at 1 Torr, the

deposition temperature was set at 400°C and the total deposition time was set to 900sec.

5.1.3 End point detection

End point control is a big challenge during a CVD process; using mass spec to detect the termination time of the process was one of the first methods for advanced process control.^{21, 56} Real-time end point process control using a mass spec sensor based metrology has been demonstrated in W SP-CVD processes. The sensor based metrology, which represents the relation between the mass spec signal and film thickness, is explained in detail in the “Training experiments to build metrologies” section of this dissertation. Before deposition, a target thickness was set in each segment. Next the integrated mass spec signal based on a pre-defined target thickness from a sensor based metrology was calculated. After the integrated mass spec signal in a specific segment reached the calculated target value, the process in that segment was terminated by only flowing 60sccm argon (60 sccm was the total gas flow rate in each segment). Meanwhile, the process in the other two segments was unchanged. Therefore, the deposition time in each segment could be different (not fixed at 900 sec). Finally, we measured the thickness obtained from four-point-probe maps of sheet resistance and compared the measurement with the target value.

5.2 Training experiments to build metrologies

5.2.1 Deliberate non uniform film deposition to build process based metrologies

Table 5- 1 lists process recipes used to deposit deliberate nonuniform films. In order to achieve high conformality via filling, we set $WF_6 : H_2 = 1 : 4$ in all process recipes.^{43,57} Since argon is an inert gas, it was used as a compensatory gas to keep the

total flow rate at 60 sccm in each segment. In Experiment (a), the flow rate of WF_6 in segment 1, segment 2 and segment 3 were 6sccm, 9sccm and 12sccm respectively. These recipe settings were cycled in Experiment (b) and Experiment (c). Post process thickness measurements were conducted by four-point-probe maps of sheet resistance. Figure 5- 1 shows the picture of the wafer from the nonuniform film deposition Experiment (a) and the thickness measurement results. From the average thickness in Table 5- 1 (Experiment (a), (b) and (c)), it was found that the greater the reactant gas concentration in a specific segment, the greater the film thickness in that segment. Although this is an expected trend, it is important to point out that with respect to the SP-CVD reactor, inter segment interactions can disturb this trend depending on the magnitude of the interactions, which in turn depends on the wafer/showerhead gap size and the reactant gases flow rate in the segments. These results match previous simulation results.^{50, 49}

Nine wafers were deposited with recipes shown in Table 5- 1. The results demonstrate a linear relationship between the W film thickness and the square root of H_2 mole fraction in each segment. Figure 5- 2 illustrates three linear models in three segments; the correlated coefficients (R^2) are higher than 88%. These models are used to select the recipe for uniform deposition or non-uniform deposition, where the process can be controlled and the film thickness can roughly be predicted.

5.2.2 Multiplexed real time mass spec sensing in W SP-CVD

There are three segments in the programmable CVD reactor; each segment experiences different CVD recipes with different parameter settings; for instance, different gas flow rates, different precursors, and different temperatures. As

mentioned before, the objective is to monitor the gas concentration in each of the three segments during a single deposition process using only one mass spec. This implies that the mass spec has to be multiplexed amongst the three segments. One challenge for multiplexed sampling is to optimize the monitoring time for each segment. The time it takes for the residual gas from the CVD reactor to reach the mass spec sensor is defined as the gas transfer time (< 1 second). The time for the mass spec sensing the gas from the sampling tube is defined as the mass spec sensing time. The total value of gas transfer time and mass spec sensing time is called the monitoring time. In the process, the connection between the mass spec sensor and the sampling tubes were cyclically switched from segment-1 to segment-2, from segment-2 to segment-3, and from segment-3 to segment-1. The monitoring time in each segment was set to be 20 seconds in every cyclic switching period.

5.2.3 Thickness metrology development

Multiplexed real-time mass spec sensing is an insight to the SP-CVD process. Figure 5- 3 shows the H_2 , HF and WF_6 mass spec signals from a typical programmable W CVD process. The monitoring time in each segment and each cycle was 20 sec and 60 sec respectively. There were 15 monitoring cycles during a single deposition process (except the end point control deposition). When the process started, the H_2 , HF and WF_6 signals increased. In the 1st cycle, the process deposited the initial W nucleation layer (reaction [1] in Chapter 2.2) which resulted in a continuous increase to the mass spec signals. From the 2nd cycle, all the gases' signals became stable, meaning the Si reduction of WF_6 was completed and the initial seed layer covered the wafer surface. Meanwhile, the H_2 reduction of WF_6 was dominant

in the W deposition process. From reaction [2] in Chapter 2.2, three moles of H₂ and one mole of WF₆ are known to produce six moles of HF and one mole of W film. During the process, both of the reactants (H₂ and WF₆) and by product gas (HF) were detected by downstream mass spec. Previous results from our group⁵⁷ showed HF provides a better metrology signal. Thus, the HF signal was selected as the metrology signal.

Figure 5- 4 reveals an *in situ* HF generation signal obtained during the programmable W CVD process. The HF baseline is the HF background signal in the SP-CVD reactor and was obtained before the process started. After the deposition started, the difference between the real-time HF signal and the HF baseline was correlated with the thickness of the W film. The metric for the W film thickness based on HF signal was defined by the following equation [4].

$$S_{HF} = \sum_{n=1}^{15} [A_{real-time}(HF) - A_{background}(HF)] \quad [4]$$

Where,

$A_{real-time}$: The area beneath the HF signal in the specific segment;

$A_{background}$: The value of the time integration of background HF signal;

n: Monitoring cycle number.

For example, as illustrated in Figure 5- 4, the area A represents the HF signal integration value from the 1st cycle in segment 2; while in the 2nd cycle, the value of the area (A+B) is represented as the integration value from the 1st two cycles (where,

area B is the HF integration value from the 2nd cycle in segment 2); as the process continued, the area C was added to area (A+B), etc. We have developed a Labview[®] program to real-time integrate the HF signal (explained in Chapter 3.5).

5.2.4 The in-situ mass spec sensor based metrologies

The normalized HF generation signals of 20 wafers were calculated according to equation [4]. A linear relationship between the W film thickness and the integrated HF signal were plotted in Figure 5- 5. A linear relationship was noticed in the metrology results from the HF signal in segment 2 and segment 3 (Figure 5- 5 (b) and (c)) with correlated coefficients (R^2) of 96.8% and 92% respectively. However, it was found that the quality of the linear fit was better in segment 2 and 3 than in segment 1; the correlated coefficient in segment 1 was around 64.9%. This was due to the limitation of the equipment. Previous experiments suggest that if the showerhead touched the wafer surface, there would be excess particle deposition around the area of contact. Therefore, a small gap (1mm) was left between the wafer and showerhead during the deposition process. However, the showerhead was not perfectly perpendicular to the wafer surface which resulted in a larger gap size over segment 1 compared to the gap sizes over segment 2 and segment 3. The gas leak from inside the showerhead to the outside area was controlled by this gap size. Hence, the leakage effect in segment 1 was higher than in other segments. Consequently, the deposition results in segment 1 showed more scattering than in the other two segments.

Based on equation [5], the average uncertainties were calculated to provide an idea for the precision of the established thickness metrology. The data is listed in Table 5- 2. The two linear metrologies (sensor based and process based) show that

segment 2 and segment 3 have a better linear fit than segment 1. The uncertainties of 1.9% ~ 4.9% were deemed sufficient for the use of a mass spec sensor based process control method.

$$Uncertainty_{Avg} = \frac{1}{n} \sum_{i=1}^n |(T_{measured} - T_{estimated}) / T_{measured}| \quad [5]$$

Where,

$T_{measured}$: Film thickness measured by 4 point probe;

$T_{estimated}$: Film thickness calculated from the linear regression fit;

n : Total wafer number (n = 20).

5.3 Demonstration of programmability --- uniform film deposition

The SP-CVD system has the unique capability to intentionally induce non-uniform films and control wafer uniformity as well.⁴⁶ In Table 5- 3 Experiment (d), the SP-CVD was reprogrammed to deposit 660nm of uniformed films in the three segments. Based on the models of Figure 5- 2, the process recipes in the three segments were reset, while other process parameters (deposition time, temperature, total pressure, etc.) were kept unchanged. A batch of 10 wafers was processed with the recipe shown in Table 5- 3. Thickness measurements showed that the average error to target in segment 1, segment 2 and segment 3 were 6.4%, 7% and 6.2% respectively. Figure 5- 6 shows the picture of the wafer from the uniform deposition Experiment (d) and the thickness measurement results.

Table 5- 1 Deliberate non uniform W film deposition recipes and thickness measurement

Experiment (a)

Segment #	1	2	3
WF₆ flow rate (sccm)	6	9	12
H₂ flow rate (sccm)	24	36	48
Ar flow rate (sccm)	30	15	0
Sqrt of H₂ mole fraction	0.63	0.77	0.89
Avg thickness (nm)	558	742	686

Experiment (b)

Segment #	1	2	3
WF₆ flow rate (sccm)	9	12	6
H₂ flow rate (sccm)	36	48	24
Ar flow rate (sccm)	15	0	30
Sqrt of H₂ mole fraction	0.77	0.89	0.63
Avg thickness (nm)	666	826	586

Experiment (c)

Segment #	1	2	3
WF₆ flow rate (sccm)	12	6	9
H₂ flow rate (sccm)	48	24	36
Ar flow rate (sccm)	0	30	15
Sqrt of H₂ mole fraction	0.89	0.63	0.77
Avg thickness (nm)	684	700	669

Table 5- 2 Comparison of the average uncertainty and standard deviation obtained from two metrologies.

	Segment 1		Segment 2		Segment 3	
	Sensor based	Process based	Sensor based	Process based	Sensor based	Process based
Uncertainty Avg.	4.1%	9.6%	1.9%	17.8%	2.1%	4.4%
Std.	4.9%	4.7%	2.4%	11.8%	2.7%	2.9%

Table 5- 3 Uniform W film deposition recipe and thickness measurement.

Experiment (d)

Segment #	1	2	3
WF₆ flow rate (sccm)	10	5	10
H₂ flow rate (sccm)	40	20	40
Ar flow rate (sccm)	10	35	10
Sqrt of H₂ mole fraction	0.82	0.58	0.82
Avg thickness (nm)	660	681	648

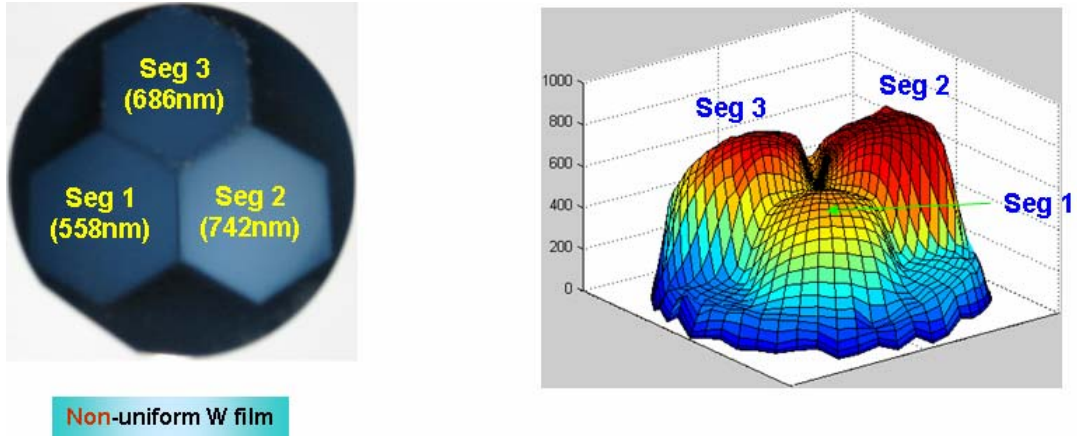


Figure 5- 1 Non-uniform W film deposition.

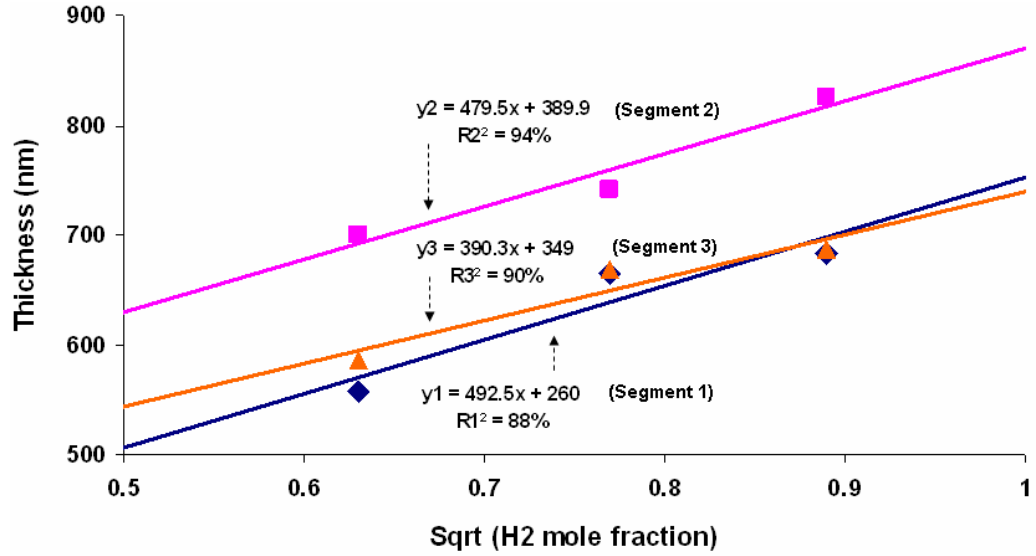


Figure 5- 2 Linear statistic model between W film thickness and square root of H₂ mole fraction.

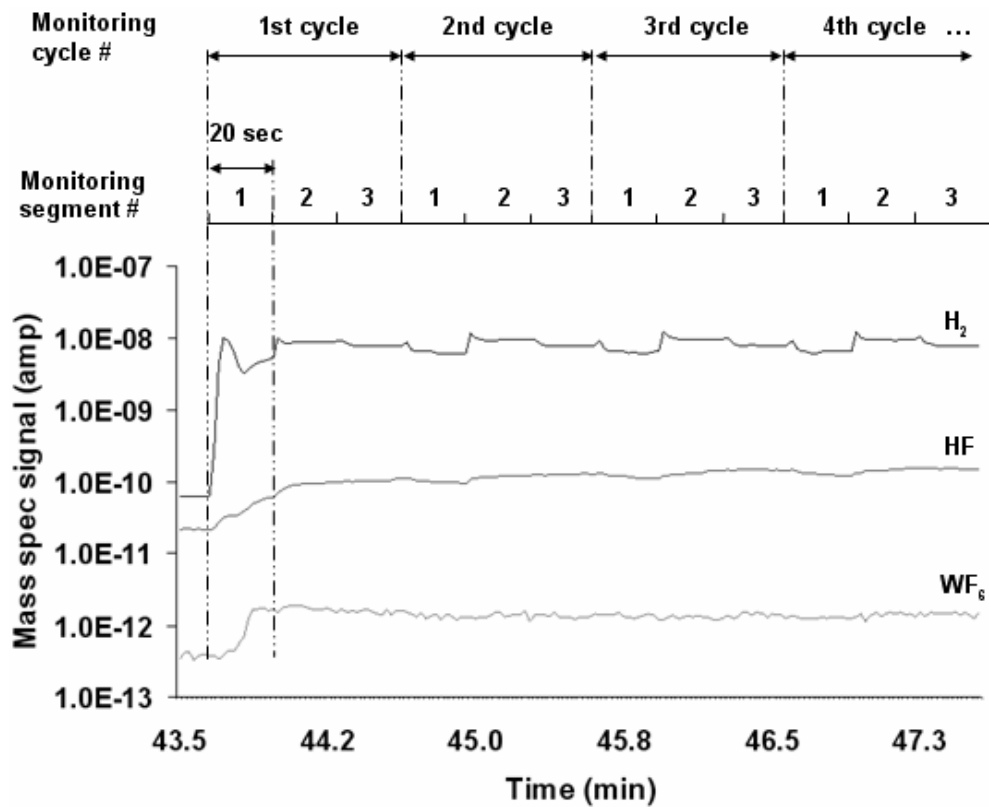


Figure 5-3 H_2 , HF and WF_6 mass spec signals from a typical programmable W CVD process. Monitoring time: 20 sec/segment; 60 sec/cycle. Typically, there are 15 cycles of monitoring during the process. This figure only illustrates the first 4 cycles of mass spec monitoring signals.

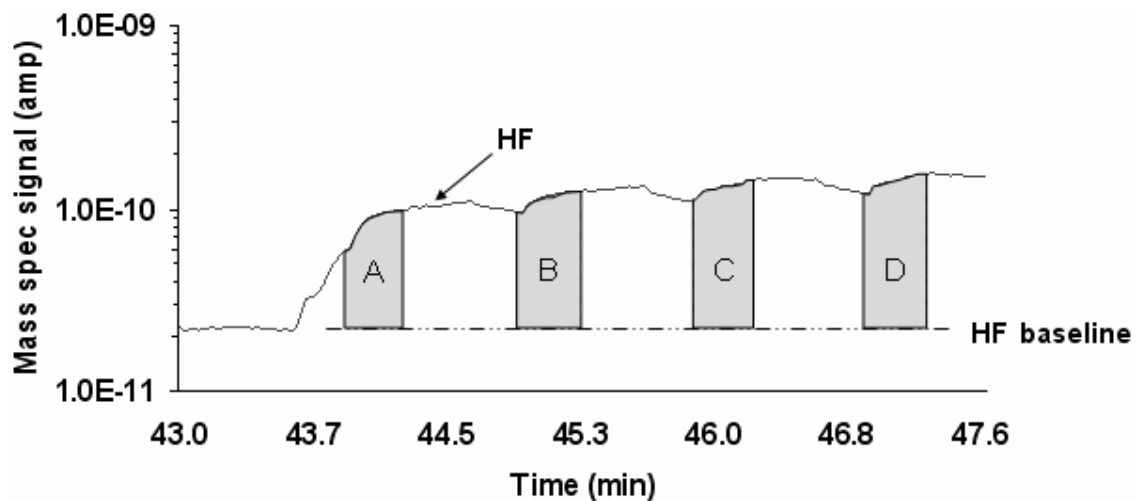
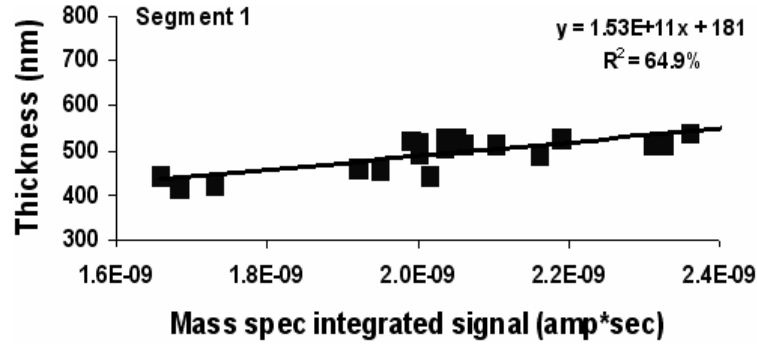
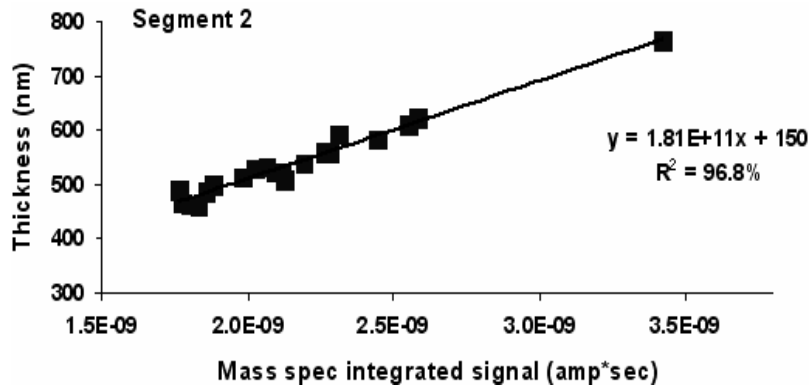


Figure 5- 4 *In situ* HF generation signal obtained in programmable W CVD process. A, B, C, D present the HF signal integration value from the 1st four cycles in segment 2.

(a)



(b)



(c)

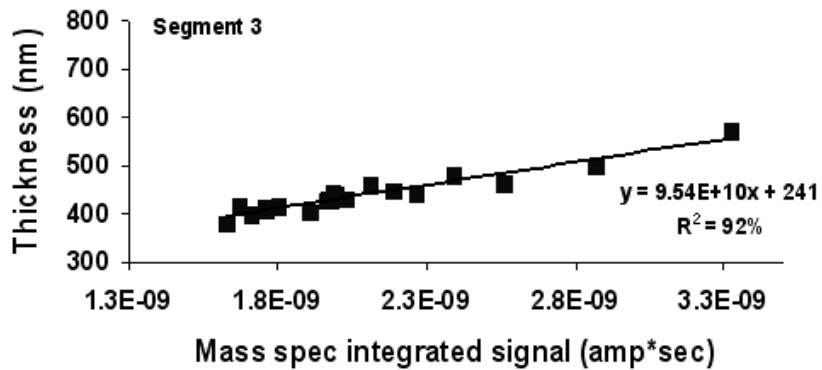
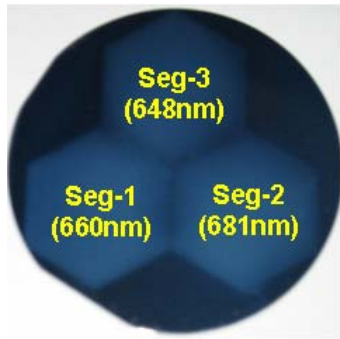


Figure 5- 5 W film thickness vs. normalized time integration of HF mass spec signal. (a) Metrology results in segment 1; (b) Metrology results in segment 2; (c) Metrology results in segment 3.



Uniform W film

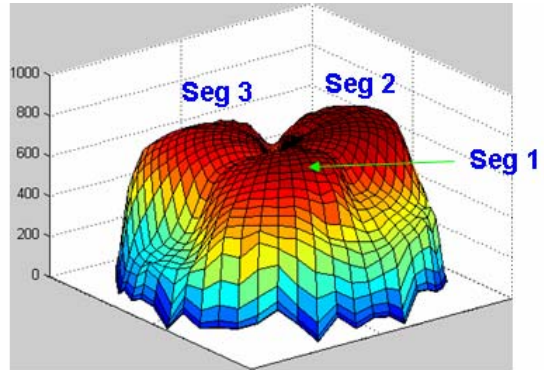


Figure 5- 6 Uniform W film deposition.

Chapter 6: Discussion

6.1 Use inter-segment gas diffusion to control the deposition gradient

The SP-CVD reactor has the unique capability of producing thin films with desired properties across the wafer and has proven to be an ideal tool for the research of combinatorial materials development.⁴⁸ Mass spec has been employed to study the gas distribution and gas transport in the SP-CVD system in order to validate the modeling of SP-CVD and to monitor the deposition process. As discussed in Chapter 4.2, the contribution of the signal from the inter-segment gas mixing from these two mechanisms can be clearly quantified. In Figure 4- 3, the mass spec signal in both Experiment 3 and Experiment 4 show that when the showerhead/wafer gap size increase, there is more inter-segment gas diffusion at the gap area. As a result, we can control the gas concentration gradient at the gap region by adjusting the showerhead/wafer gap size. As shown in Figure 4- 2, by comparing the value of A and B it is found that B is almost half of A. This was due to the feed gas flow rate in Figure 4- 2 (b) being reduced to half of the feed gas flow rate in Figure 4- 2 (a). A high gas feeding rate prevents more gas diffusion from both the common exhaust port (ISM-BD) and the showerhead/wafer gap area (ISM-wafer). This result indicates that another method to control the gas concentration distribution above the wafer is to change the feed gas flow rate. Therefore, in the future, deposition gradients can be controlled by adjusting the feed gas flow rate as well as the gap size between the wafer surface and the bottom of the segmented showerhead.

6.2 Mass spec signal variations in different segments

One of the main novelties of the multiplexed mass spec sensing system is that one mass spec is used for real time *in-situ* monitoring of all three segments of a CVD process to conduct process/equipment diagnosis and to perform leak checks at the common exhaust port and the precursor source area. The mass spec data from the three segments reveal a signal difference between segments even when all three segments have the same gas flow rates. In Figure 6- 1: an H₂ signal ratio of segment-1 : segment-2 : segment-3 as 1.1 : 1.3 : 1. As shown in Figure 3- 2, there are many connection devices between the CVD reactor and the mass spec, such as, orifice, sampling tube, valve, and flexible tube. There is some variation in these connections from one segment to another. The tolerance of orifice 1 (35μ orifice flow rate tolerance ±10%),⁵⁸ the conductance of the valve, and the length of the flexible tube are the main factors that affect the total conductance of each sampling tube causing the mass spec signal to have differences between segments. The signal ratio between segments also depends on the gas type. In Figure 6- 1 we find that the Ar signal ratio of segment-1 : segment-2 : segment-3 is 1.2 : 1.5 : 1, which is different from the H₂ signal ratio. The reason for this difference is we use a turbo molecular pump to keep the mass spec working at a low pressure and the pumping speed of Ar is higher than H₂ because Ar's compression ratio is higher than H₂'s compression ratio. As a result, the signal ratio between segments depends on the type of gas. We believe the signal differences between segments can be reduced if the variation of hardware configuration between segments can be reduced.

We have developed a film thickness metrology, which reflects the relation between the mass spec signal and the film thickness which will allow us to do end point detection in SP-CVD process. In order to solve the problem of signal variation between segments, we have developed a model-based metrology for each segment and have further applied the metrology to control the process in the correlative segment.

6.3 Transient peak in the mass spec signal

6.3.1 Origin of the transient peak

Each sampling tube was coupled with a bypass line. During idling status (not monitoring status), most of the gas in the sampling tube was pumped out through the bypass line. However, because the pumping speed of turbo pump 2 (in Figure 3- 3) is lower than that of turbo pump 1 (in Figure 3- 3), a little gas still remained in the sampling tube and the valve area. The transient peak seen in Figure 6- 1 is the signal of the gas cumulated in the sampling tube and the valve. Once the valve was opened, the cumulated gas was first sensed by QMS. After the cumulated gas was pumped out by the turbo pump (which was connected with the QMS chamber), the mass spec signal reached a stable value. The transient time is different with different gases, our test results are summarized in Table 6- 1. The transient peak can be reduced if the pumping speed of turbo pump 2 is same as the pumping speed of turbo pump 1, since no gas will be cumulated at the sampling tube and the valve area.

6.3.2 Transient peak vs. the precision of mass spec based metrology

The transient peak is one reason that caused the error of the mass spec based metrology. As described in Chapter 3.5, the SP-CVD sensing algorithm (executed by

a Labview[®] VI module) separates and integrates the mass spec signal for each segment. The signal from the transient peak is also included in the integrated signal value. In the future, if the turbo pump 2 is replaced by a pump with the same pumping speed of turbo pump 1, the transient peak effect will be reduced and the precision of mass spec based metrology will be increased. For example, if the SP-CVD system has 10 segments, in order to get more sampling data during the process, the monitoring time of each segment will be decreased. However, the monitoring time should be longer than the transient time, therefore, if the transient time can be decreased, the monitoring time in each segment can also be decreased. Hence, reducing the effect of the transient peak will be more important for the more segment design in the next generation of SP-CVD system.

6.3.3 Remove the transient signal by SP-CVD sensing VI

We can avoid integrating the transient signal by changing the starting time for the signal integration. The transient time of HF is around 5 seconds (if HF concentration is very low, the transient time will be shorter). So we can change the program of SP-CVD sensing VI and make it to start integrating 5 seconds later after it receives the mass spec signal in a specific segment. This is also a future work we are still working on.

6.4 Non-uniform heating effect and programmability of SP-CVD

All experimental results revealed that the W film in segment 2 was significantly thicker than that in segment 1 and segment 3 even though the same gas flow rates were introduced in all segments. This is caused by the non-uniform heating effect in different segment. As shown in Figure 6- 3, a spirally shaped substrate heater

was used to heat the wafer during the deposition. Because there are more heater coils in segment 2 region than that in other segments region, the temperature in segment 2 region is much higher. This nonuniform heating is considered to be a process disturbance. The SP-CVD system is capable to re-program the process by adjusting the gas flow rates in three segments to deposit the desired film across the whole wafer surface (either uniform films or deliberate non-uniform films). This is also an effective way to prove the programmability of this novel SP-CVD system.

6.5 Sensor based metrology vs. process based metrology

Comparing the data from the mass spec sensor based metrology and the process based metrology (as indicated in Table 5- 2), it was determined that the mass spec controlled metrology shows better precision with lower values of uncertainties and standard deviations in all three segments. This is apparent in segment 2, where the uncertainty was reduced from 17.8% to 1.9% after applying the mass spec sensor based metrology.

The process based metrology was developed based on the relationship between the equipment and process parameters on one hand and the film thickness on the other. This is strongly related to the process stability and equipment performance, and more specifically to how actual process conditions reflect the equipment settings. When we conducted training experiments to build this process based metrology, some process/equipment variations occurred, for example, the performance of mass flow controller and valves are different between the different processes.

In contrast, the sensor based metrology was built based on the byproduct gas signal from the process and the film thickness. Because CVD reaction is a

stoichiometric chemical reaction, in our W CVD process, the amount of byproduct gas HF is always proportional to the amount of deposited W film. In a sense, therefore, the sensor based metrology has in principle the advantage that it detects the actual process condition at the wafer, not the equipment settings intended to achieve the process condition at the wafer. This principle has paved a way for us to develop a mass spec sensor based film thickness metrology with a better precision. These results suggest that in future combinatorial material studies, the process recipe will be selected based on the process based metrology. This helps determine whether the deposited film will be uniform or nonuniform with the selected recipe. Second, during the process, the sensor based metrology will be applied to accurately control the process in real-time: (1) to determine the time to terminate the process; (2) to predict the film thickness.

6.6 The accuracy of end point control

A total of five wafers were processed to test the capability of end point control in the SP-CVD process. The detailed data is summarized in Table 6- 2 and the results are depicted in Figure 6- 2. Compared to previous research results,^{27, 51} the average error (5% ~ 10%) and standard deviation (7% ~ 13%) from the SP-CVD processes were higher. This was due to several reasons: (1) the extremely low conversion rate of H₂ (~3%) in the H₂ reduction process; and (2) interference from neighboring segments (ISM-wafer and ISM-BD). Better end point control performance is expected if the conversion rate is improved to a high conversion rate (~50% in high volume manufacturing industry). Increasing the process pressure and replacing the high reaction conversion reactant (such as SiH₄) can improve the process conversion

rate. Moreover, it is believed that the interference effect from neighboring segments can be decreased if the inter-segment gas diffusion is decreased.⁵⁹ The basic approach to reducing the neighboring interference includes increasing the gas flow rate in each segment and using the isolated down stream pumping system for each segment.

Figure 6- 2 reveals that most of (>73%) the films are thicker than the target value. Root cause investigations indicate that the inter-segment gas diffusion and the precursor delivery system design are two main reasons that caused this error.

6.6.1 Inter-segment gas diffusion

As discussed in Chapter 4.1, there are two mechanisms of inter-segment gas diffusion: ISM-wafer and ISM-BD. These two types of inter-segment gas diffusion affect the precision of the end point detection. For instance, during the end point control experiment, the process in segment 1 first reached the target value. The process in segment 1 was terminated by flowing only argon in that segment. At the same time, the process parameters in the other segments were not changed. The HF gas concentration in segment 1 was decreased since there was no reaction gas to produce HF in segment 1. Therefore, the byproduct HF in the other two segments diffused into segment 1 and caused the integrated HF signal in segment 2 and segment 3 to be lower. When the integrated HF signal in the other two segments reached the target value, the deposited films were actually thicker than the pre-defined target thickness. Increasing either process pressure or gas flow rates can reduce the effect of inter-segment gas diffusion and increase the accuracy of end point control in SP-CVD.

6.6.2 Precursor delivery system design

The second reason is from the SP-CVD precursor delivery system design limitation, where the control valves of the precursors are installed out of the reactor. However, the distance between the valve and the end of the gas feed tube is around 35 inches. When the process was terminated, the residual gases, which were left in the tubes between the valve and the end of the gas feed tube could still flow into the SP-CVD reactor and deposit films. This post-process deposition resulted in thicker films. The next generation of equipment design may apply MEMS based micro valves at the end of the gas feed tubes; thereafter, the post-process deposition problem can be solved and the precision of end point detection in SP-CVD will be increased.

Table 6- 1 Transient time for different gases

Gas	H ₂	HF	Ar	WF ₆
Transient time (sec)	4.5	5	17	5

Table 6- 2 SP-CVD end point detection experiment data and statistical analysis results.

Wafer #	Segment-1 (nm)		Segment-2 (nm)		Segment-3 (nm)	
	Target	Measurement	Target	Measurement	Target	Measurement
1	590	610	722	727	543	559
2	558	507	630	643	489	430
3	578	634	620	680	495	590
4	597	672	672	688	509	543
5	528	585	644	579	476	422
Avg. Error	8.61%		5.05%		10.35%	
Std. of error	8.72%		7.33%		12.82%	

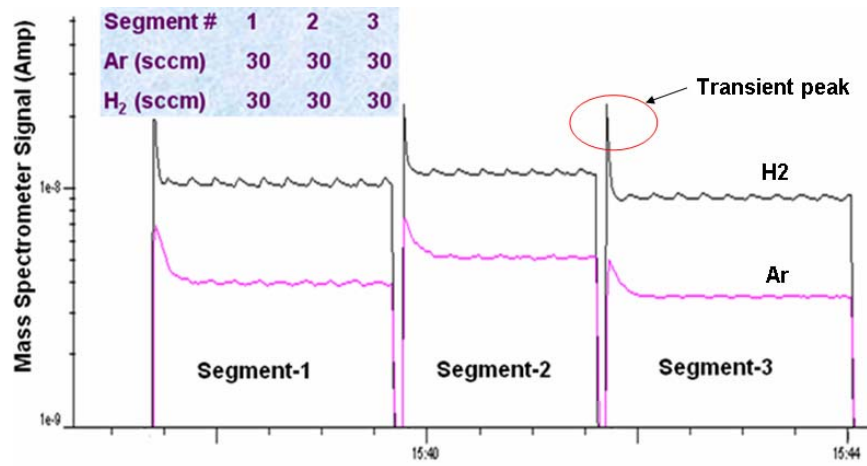
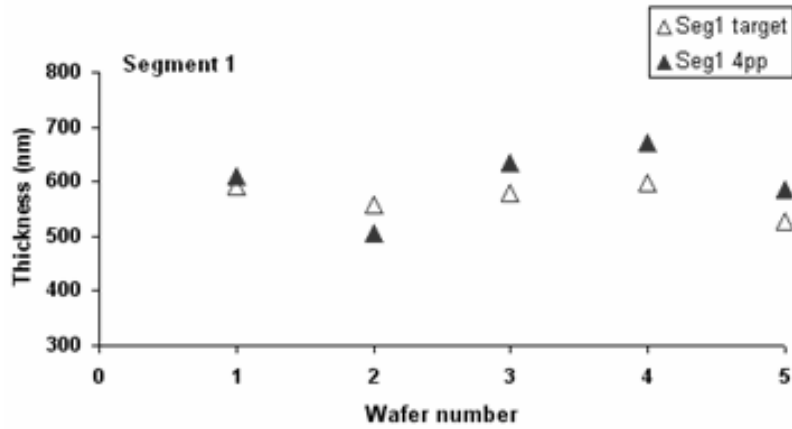
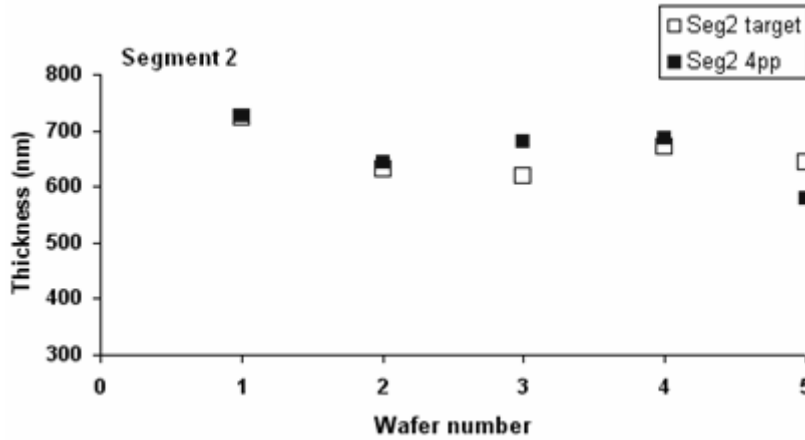


Figure 6- 1 Mass spec signal from different segment.

(a)



(b)



(c)

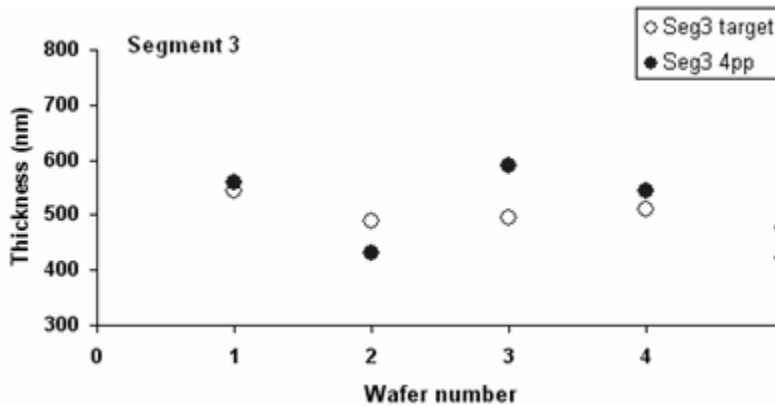


Figure 6- 2 Plots showing target thickness data from sensor based metrology vs. experimental thickness data measured by 4PP after the experiments were stopped by end pointing using multiplexed mass spec for 5 wafers.



Figure 6- 3 Substrate heater: more heater coils in segment-2 area.

Chapter 7: Conclusion and future work

7.1 Multiplexed mass spec sensing in SP-CVD

A multiplexed spatially resolved mass spec sensing system has been implemented for a spatially programmable CVD system. A simulation model has been designed to find the best parameters in the pressure transduction sampling system design. Based on the simulation results, a 35 μm orifice sampling tube coupled with a bypass line is a primary approach to reduce the process pressure (~ 1 Torr) to a low pressure (10^{-6} Torr). This novel design has given the mass spec the ability to perform multiplexed real time *in-situ* monitoring of a CVD process in three segments with a short gas transfer time (1 sec), a key factor to achieve multiplexed real-time chemical sensing.

Experimental results have demonstrated the two mechanisms of inter-segment gas mixing: (1) gas diffusion through the gap between the showerhead and wafer (ISM-wafer); (2) back diffusion from the common exhaust port (ISM-BD). These two types of gas diffusion affect the gas distribution in each segment. Mass spec has been used to experimentally validate the gas distribution at different vertical positions within one segment. The results from the mass spec show consistent trends with the simulation result taken from the model. From the mass spec signal, the amount of the signal from the gas diffused from other segments can be quantified and used to understand gas transport in the programmable CVD system. It is important to understand the fundamental phenomena associated with the reactor design and its capability to form mass spec sensor based metrology for future research of

combinatorial materials research.⁶⁰ The asymmetrical design of the equipment into three segments will not affect the SP-CVD process control. A sensor based metrology of each segment has been established and applied to real-time control of the deposition process in each segment.

7.2 Multiplexed mass spec based thickness metrology and process control

Spatially resolved mass spec sensing has been successfully used to monitor SP-CVD process *in situ* and in real-time. A W SP-CVD process using H₂ reduction of WF₆ was performed to deposit across-wafer uniform films and deliberate non-uniform films. Thickness metrology based on the normalized HF mass spec signal was developed for each segment. The average accuracies of 1.9% ~ 4.4% were obtained from the linear models between the integrated mass spec HF signal and the post-process thickness measurements.

Multiplexed mass spec based thickness metrology has been applied to demonstrate the capability of end point detection in W SP-CVD processes. Film thickness can be estimated during the process. The average error of the end point detection approaches 5% at the best case. A better metrological precision can be expected if the process conversion rate is increased and the design of the precursor delivery system is improved.

Although intra-segment uniformity is also very important, this work has concentrated on real-time control of the inter-segment uniformity or nonuniformity by multi-point mass spec sensing. Intra-segment uniformity is under study, and results will be reported in future publications.⁶¹

Future research includes working on the deposition with a larger gap size between the wafer and showerhead (3mm, 5mm...) in order to investigate the relationship between the gap sizes, film growth rate and mass spec signal. Moreover, exploration of new research directions, such as spatially programmable atomic layer deposition (SP-ALD) of high K material (SiO_2 , Al_2O_3 ...) and the sensor based metrology in SP-ALD, and more segmented showerhead design are being investigated. This research is paving the way for guiding rapid reprogramming of film deposition process for future combinatorial materials research.

Bibliography

¹ Gary W. Rubloff, Proc. 2003 International Conference on Characterization and Metrology for ULSI Technology, Austin, TX, March 24-28, 2003, ed. by D. G. Seiler et. al., AIP Conf. Proc. Vol. 683, ISBN 0-7354-0152-7 (AIP, Melville NY , 2003), 583-591.

² 1994 National Technology Roadmap for Semiconductors, section on Materials and Bulk Processes, and 1994 Metrology Supplement to the National Technology Roadmap for Semiconductors, section on Sensors and Methodology for In Situ Process Control.

³ S. W. Butler, J. Vac. Sci. Technol. B Vol. 13, pp. 1917-1923 1995.

⁴ S. W. Butler, J. Hosch, A.C. Diebold, and B.V. Eck, Future Fab International 1, 315 (1997).

⁵ K S C Kuang and W J Cantwell, INSTITUTE OF PHYSICS PUBLISHING, Smart Mater. Struct. 11 (2002) 840–847.

⁶ Hughes, C.; Van Hoeymissen, J.A.B.; Heyns, M.; *In*: 1999 IEEE International Symposium on Semiconductor Manufacturing Conference Proceedings (Cat No.99CH36314). Piscataway, NJ, USA: IEEE, 1999. p. 209-12.

⁷ Xi Li, Marc Schaepekens, and Gottlieb S. Oehrlein, J. Vac. Sci. Technol. A, vol. 17, pp. 2438-2446, 1999.

⁸ L. Lieszkovszky, A. R. Filippelli, and C. R. Tilford, J. Vac. Sci. Technol. A, vol. 8, pp. 3838-3854, 1990.

⁹ G. G. Barna, L. M. Loenstein, R. Robbins, S. O'Brien, A. Lane, D.D. White, Jr., M. Hanratty, J. Hosch, G. B. Shinn, K. Taylor, and K. Branker, *IEEE Trans. Semiconduct. Manufact.*, vol. 7, pp. 149-157, 1994.

¹⁰ G. G. Barna, L. M. Loewenstein, K. J. Brankner, S. W. Butler, P. K. Mozumder, J. A. Stefani, S. A. Henck, P. Chapados, D. Buck, S. Maung, S. Saxena, and A. Unruh, J. Vac. Sci. Technol. B Vol. 12, pp. 2860-2867, 1994.

¹¹ D. F. Marran, C. M. Nelson, L. J. Guido, and B. Gaffey, in Proc. SPIEInt. Soc. Opt. Eng. USA, 1999, pp. 24–31.

¹² S. Salim, C. A. Wang, R. D. Driver, and K. F. Jensen, J. Cryst. Growth 169, 443 (1996).

-
- ¹³ Z.-H. Zhou, S. Compton, I. Yang, and R. Reif, *IEEE Trans. Semiconduct. Manufact.*, Vol. 7, pp. 87-91, 1994.
- ¹⁴ L. Henn-Lecordier, J. N. Kidder, Jr., and G. W. Rubloff, *J. Vac. Sci. Technol. B*, Vol. 21, 1055-1063, 2003.
- ¹⁵ L. Henn-Lecordier, J.N. Kidder, Jr., and G.W. Rubloff, *J. Vac. Sci. Technol. A*, Vol. 22, 1984-1991, 2004.
- ¹⁶ K. C. Lin, IEEE/SEMI Advanced Semiconductor Manufacturing Conference, pg. 440-445, 1999.
- ¹⁷ M. B. Naik, W.N. Gill, R.H. wentorf, R.R. reeves, *Thin Solid Films* 262 (1995)60-66.
- ¹⁸ B. Zheng et al. *Materials Chemistry and Physics* 41 (1995) 173-181.
- ¹⁹ Theodosia Gougousi, Yiheng Xu, Jonn N. Kidder, Gary W. Rubloff, *J. Vac. Sci. Technol. B*, vol. 18, pp. 1352-1363, 2000.
- ²⁰ T. Michael Banks, Gregory R. Diamond, Scott J. Ruck, "Intergrating mass spectrometry data into the fab environment", *Semiconductor International*; Jun 1997; 20, 6; ABI/INFORM Global pg.137-145.
- ²¹ Robert K. Waits, *J. Vac. Sci. Technol. A*, Vol. 17, No. 4, pp. 1469-1478, 1999.
- ²² Laura Peters, *Semiconductor International*; Oct 1997; 20, 12; ABI/INFORM Global, pg. 94.
- ²³
- ²⁴ D. W. Greve, T. J. Knight, X. Cheng, B. H. Krogh, M. A. Gibson, and J. LaBrosse, "Process control based on quadropole mass spectrometry", *J. Vac. Sci. Tech. B*, vol. 14-1, pp. 489- 493, 1996.
- ²⁵ Thomas J. Knight, David W. Greve, Xu Cheng, and Bruce H. Krogh, *IEEE TRANSACTIONS ON SEMICONDUCTOR MANUFACTURING*, VOL. 10, NO. 1, P137-146, FEBRUARY 1997.
- ²⁶ T. Gougousi, R. Sreenivasan, Y. Xu, L. Henn-Lecordier, J.N. Kidder, Jr., G. W. Rubloff,, and E. Zafiriou, *Characterization and Metrology for ULSI Technology: 2000 International Conference*, Gaithersburg, MD, 26-29 June 2000, AIP Conference Proceedings, Melville, NY, 2001, vol. 550, pp. 249-253.
- ²⁷ Y. Xu, T. Gougousi, and G. W. Rubloff, *J. Vac. Sci. Technol. B*, vol. 20, pp. 2351-2360, 2002.

-
- ²⁸ Yiheng Xu, Ph.D thesis 2000, REAL-TIME IN-SITU CHEMICAL SENSING, SENSOR-BASED FILM THICKNESS METROLOGY, AND PROCESS CONTROL IN W-CVD PROCESS. Page 38.
- ²⁹ James Barker, David J. Ando, Reginald Davis, Martin J. Frearson, Mass Spectrometry (John Wiley & Sons, New York, 1999), p. 1-2.
- ³⁰ M.R. Walsh, M.A. LaPack, ISA Transactions 34 (1995) 67-85.
- ³¹ INFICON TRANSPECTOR[®] 2 Gas Analysis System Manual, 1998.
- ³² H. W. Werner and A. J. Linssen, J. Vac. Sci. Technol. 11, 843 (1974).
- ³³ E. K. Broadbent and C. L. Ramiller, J. Electrochem. Soc. 131, 1427 (1984).
- ³⁴ E. K. Broadbent and W. T. Stacy, Solid State Technol. 28, 51 (1985).
- ³⁵ *Proceeding of the 1987 Workshop on Tungsten and other Refractory Metals for VLSI Applications*, edited by V. A. Well (Materials Research Society, Pittsburgh, PA, 1988).
- ³⁶ K.J. Kuijlaars, C.R. Kleijn, H.E.A. van den Akker, Thin Solid Films 270 (1995) 456-461.
- ³⁷ Ming L. Yu, Benjamin N. Eldridge, J. Vac. Sci. Tech. A. vol. 7, pp. 625-629, 1989.
- ³⁸ E. K. Broadbent and W. T. Stacy, Solid State Technol. 28, 51 (1985).
- ³⁹ Yiheng Xu, Ph.D thesis 2000, REAL-TIME IN-SITU CHEMICAL SENSING, SENSOR-BASED FILM THICKNESS METROLOGY, AND PROCESS CONTROL IN W-CVD PROCESS. Page 88.
- ⁴⁰ Jory A. Yarmoff and F. Read Mcfeely, J. App. Phys. Vol. 63, pp. 5213-5219, 1988.
- ⁴¹ K. Y. Tsao and H. H. Busta, J. Electrochem. Soc. 131, 2702 (1984).
- ⁴² R. Sreenivasan, T. Gougousi, X. Yiheng, J. Kidder, E. Zafiriou, and G. W. Rubloff, J. Vac. Sci. Technol. B 19, Pg. 1931-1941, 2001.
- ⁴³ Julian J. Hsieh, J. Vac. Sci. Tech. A, vol. 11, pp. 3040-3046, 1993.
- ⁴⁴ Julian J. Hsieh, J. Vac. Sci. Tech. A, vol. 11, pp. 78, 1993.
- ⁴⁵ J. J. Hsieh and R. V. Joshi, in *Advanced Metallization for ULSI Applications*, edited by V. V. S. Rana, R. V. Joshi, and I. Ohdomari (Materials Research Society, Pittsburgh, PA, 1992), p. 77.

-
- ⁴⁶ Choo, J. O., R. A. Adomaitis, L. Henn-Lecordier, Y. Cai, and G. W. Rubloff, *Rev. Sci. Instrum.* 76, 062217 (2005).
- ⁴⁷ Raymond A. Adomaitis, John N. Kidder, Jr., and Gary W. Rubloff, **U.S. Patent No. 6,821,910**, issued Nov. 23, 2004.
- ⁴⁸ Jae-Ouk Choo; Adomaitis, R.A.; Rubloff, G.W.; Henn-Lecordier, L.; Yuhong Cai; American Control Conference, 2004. Proceedings of the 2004 Volume 1, 30 June-2 July 2004 Page(s):287 - 292 vol.1.
- ⁴⁹ Jae-Ouk Choo, Ph.D. Proposal, 2002, Development of Spatially Controllable Chemical Vapor Deposition System.
- ⁵⁰ Jae-Ouk Choo, Raymond A. Adomaitis, Gary W. Rubloff, Laurent Henn-Lecordier, and Yijun Liu, *AIChE J.* 51 (2) 572-584 (Feb 2005).
- ⁵¹ Soon Cho, Laurent Henn-Lecordier, Yijun Liu, and Gary W. Rubloff, *J. Vac. Sci. Technol. B*, vol. 22, pp. 880-887, 2004.
- ⁵² John F. O'Hanlon, *A user's guide to vacuum technology*, 3rd edition, (A JOHN WILEY & SONS, INC.), pg. 153.
- ⁵³ A. Roth, *Vacuum Technology*, third, updated and enlarged edition, (ELSEVIER SCIENCE PUBLISHERS B.V.), pg. 84.
- ⁵⁴ Xi Li, Gottlieb S. Oehrlein, Marc Schaeplen, Robert E. Ellefson, Louis C. Frees, *J. Vac. Sci. Technol. A*, vol. 21, pp. 1971-1977, 2003.
- ⁵⁵ Walter Umrath, *Fundamentals of vacuum Technology*, Inficon, 1998
- ⁵⁶ B. A. Raby, *J. Vac. Sci. Technol.* 15, 205 (1978).
- ⁵⁷ Theodosia Gougousi, Yiheng Xu, John N. Kidder, Gary W. Rubloff, Charles R. Tilford, *J. Vac. Sci. Technol. B*, vol. 18, pp. 1352-1363, 2000.
- ⁵⁸ Lenox laser tubing orifice catalog.
- ⁵⁹ Y. Cai, R. Sreenivasan, J.O. Choo, L. Henn-Lecordier, and R. A. Adomaitis, and G. W. Rubloff, **MULTIPLEXED MASS SPECTROMETRIC SENSING IN A SPATIALLY PROGRAMMABLE CHEMICAL VAPOR DEPOSITION REACTOR**, to be submitted to *JVST B* 2005.
- ⁶⁰ Y. Cai, R. Sreenivasan, L. Henn-Lecordier, R. A. Adomaitis, and G. W. Rubloff, "Real-time multiplexed mass spectrometry sensing and thickness metrology in a

tungsten spatially programmable chemical vapor deposition process”, to be submitted to JVST B 2005.

⁶¹ R. Sreenivasan, R. A. Adomaitis, and G. W. Rubloff, “A Demonstration of Spatially Programmable Chemical Vapor Deposition: Model-Based Uniformity/Non-uniformity Control”, to be submitted to JVST B 2006.